Multivalent T cell Engagers for Cancer Therapy

DEVELOPING MULTIVALENT T CELL ENGAGERS TOWARDS LOCAL CANCER
IMMUNOTHERAPIES

By April Marple, B.Sc.

A Thesis Submitted to the School of Graduate Studies in Partial Fulfilment of the
Requirements for the Degree Master of Science

TITLE:	Developing Multivalent T Cell Engagers towards local cancer immunotherapies
AUTHOR:	April Marple, B.Sc. (University of Waterloo)
SUPERVISOR:	Dr. Ryan Wylie
NUMBER OF PAGES:	74

LAY ABSTRACT

Drugs that focus on engaging the patient's immune system (immunotherapy) to target and kill cancerous cells offer a more effective and personalized path to cancer treatment. Many of these drugs have been designed for intravenous delivery and this has unfortunately created a short residence time in the body, lowering efficacy against solid tumors. High intravenous doses are needed to achieve efficacy, which often results in unwanted and potentially lethal toxicity. To improve this, re-designing the drugs for local delivery (i.e., intratumoral), would limit systemic toxicity while improving efficacy against solid tumors. Here, we develop a new scaffold for immunotherapeutics with improved retention at injection sites, in addition to being easy to fabricate, and tailor for different cancer targets.

ABSTRACT

Immunotherapeutics that redirect the immune system toward cancerous cells have been extensively researched over the past decades. T cell engagers, such as BiTEs, are moving through clinical trials for many types of cancers. However, their small hydrodynamic radius and lack of Fc mediated recycling results in short plasma half-lives upon intravenous administration, which prevents the achievement of minimum effective concentrations in solid tumors. The local administration of T cell engagers provides a method to achieve therapeutic concentrations in tumor tissue. Herein, we developed a new T cell engager scaffold optimized for local delivery by increasing the size of the conjugate to extend tissue residence time and established a synthetic protocol to rapidly exchange the cancer targeting ligand towards addressing tumor heterogeneity. Redesigning T cell engagers for local administration utilized a full anti-CD3 antibody modified with short ethylene oxide $((EO)_x)$ linkers for the grafting of cancer targeting peptides. Additionally, creating a scaffold using SPAAC-based conjugation allows for rapid fabrication of multivalent T cell engagers (MuTEs) for many cancers, utilizing an already existing library of cancer targeting peptides. Ideal grafting densities for short ethylene oxide $((EO)_x)$ linkers were determined and tested *in vitro* in PSMA positive and HER2 positive cancer cell lines. In a local delivery *in vitro* model using embedded PSMA expressing spheroids, MuTEs resulted in greater cancer spheroid killing compared to traditional bispecific T cell engagers (BiTEs) over a 2-week period, with 2.5-fold greater cytotoxicity with MuTEs than BiTEs after 12 days. MuTEs have the potential to improve efficacy of T cell engagers for local delivery applications and offer a simplified synthetic pathway to develop a library to T cell engagers that target various cancer cell antigens.

ACKNOWLEDGEMENTS

Table of Contents

LIST OF FIGURES AND TABLES

LIST OF ABBREVIATIONS

^{1}H-NMR: Proton nuclear magnetic resonance

Ab: Antibody

aCD3: Antibody to cluster of differentiation 3

APC: Antigen presenting cell

APMA: Aminopropyl methacrylamide

Az: Azide

BiTE: Bispecific T cell Engager

CB: Carboxybetaine methacrylamide

CD3: Cluster of differentiation 3

CTP: Cancer targeting peptide

DBCO: Dibenzocyclooctyne

DCM: Dichloromethane

DMEM: Dulbecco's Modified Eagle Medium

DMF: Dimethylformamide

EO_x: Ethylene oxide oligomers (with x repeat units)

E:T: Effector to Target ratio

F_{AB}: Antigen binding fragment

FBS: Fetal bovine serum

GPC: Gel permeation chromatography

GUL: Glutamate urea lysine

GUL-Az: Azide modified glutamate urea lysine

HA: Hyaluronic acid

HEK-PSMA: PSMA over-expressing HEK293 embryonic kidney cell line

HEPG2: PSMA negative liver cancer cell line

kDa: Kilodalton

LNCaP: PSMA positive prostate cancer cell line

MALDI-TOF: Matrix assisted laser desorption/ionization – time of flight

MeOH: Methanol

M_n: Number average molecular weight

MuTE: Multivalent T cell Engager

MW: Molecular weight

MWCO: Molecular weight cut-off

NAAG: *N*-Acetyl-L-aspartyl-L-glutamate

NHS-DBCO: N-hydroxysuccinimide dibenzocyclooctyne

NHS-EO-DBCO: N-hydroxysuccinimide-polyethylene glycol-dibenzocyclooctyne

PBMC: Peripheral blood mononuclear cells

P(EG)$_x$MA: poly(ethylene glycol)$_x$ methyl ether methacrylate

PBS: Phosphate buffered saline

pCB: poly-carboxybetaine methacrylamide

pCB-APMA: poly-carboxybetaine-co-aminopropyl- methacrylamide

PEG: polyethylene glycol

PSMA: Prostate specific membrane antigen

ScFv: Single chain variable fragment

SDS: Sodium dodecyl sulfate

SPAAC: strain-promoted azide-alkyne cycloaddition

TAA: Tumor associated antigen

TCR: T cell receptor

DECLARATION OF ACADEMIC ACHIEVEMENT

All cell lines were transduced with luciferase or iRFP by Neil Savage. Prostate and HER2 targeting ligands, and PSMA BiTE were received from the Rullo lab. Binding data was collected and analyzed by Alex Jesmer. All other data collection and interpretation were performed by the author with insight and support from Alex Jesmer and Dr. Ryan Wylie.

Chapter 1 - Introduction

1.1   Rationale

Immunotherapeutics are a rapidly growing field of interest for cancer treatment over the past decades. Specifically, immunotherapeutics called T cell engagers have revolutionized the field of cancer immunotherapies[1] and been used in combination therapies with other classes of immunotherapeutics, such as CAR-T and checkpoint blockades.[2,3] The development of a Bispecific T cell Engagers (BiTEs) for the treatment of B cell lymphoma led to a large assortment of BiTEs for cancer treatments. In clinical trials, the limitations of BiTEs were discovered and since then similar constructs have been developed aimed to improve the BiTEs. The limitations regularly addressed by new T cell engagers include (1) low plasma half-life, (2) poor solid tumor efficacy, and (3) immune escape by antigen loss. However, many of these constructs have been complex in design and synthesis, resulting in limited clinical application, or did not improve accumulation in solid tumors without significant systemic side effects. One recurring problem for BiTEs and other similar T cell engagers is their fast elimination rate from the body, often preventing the achievement of therapeutic concentrations, resulting in the need for higher doses that lead to potentially fatal systemic toxicity.[4]

The local administration of immunotherapeutics at the tumor site has shown promise in the treatment of primary and distal tumors. Although, because BiTEs were designed for intravenous administration, BiTE structures were not optimized for local delivery. BiTEs are typically designed as smaller structures (two linked scFvs) for

improved tissue penetration, but the smaller protein size also increases clearance rates.[5] Moreover, to target tumor heterogeneity, BiTEs require significant investment for the development of different antigen targeting structures. Redesigning the T cell engager construct for local delivery would allow for improved control in antigen targeting, reduced systemic toxicity, and maintenance of therapeutic concentrations within tumor tissues.[6,7] As well, finding a way to easily modify the construct to target different cancer antigens, utilizing an already existing library of cancer targeting peptides, would help to address tumor heterogeneity. Overall, designing a simple to synthesize, longer lasting tissue residence, and modular targeting system for T cell engagers for local delivery would be beneficial to the field.

1.2   Thesis Objectives

The purpose of this thesis is to develop, characterize, and optimize Multivalent T cell engagers (MuTEs) to improve the efficacy of T cell engagers for local delivery applications by increasing molecular weight got improved tissue residence time and establishing a modular synthetic protocol to easily address tumor heterogeneity. Specifically, development of MuTEs will meet the following objectives:

1. Redesign of BiTEs for a local administration to improve retention and extend the duration of therapeutic concentrations at the disease site;

2. Establish a simple and modular synthetic protocol with copper-free click chemistry (SPAAC) for efficient and rapid fabrication of T cell engagers; and,

3. Establish a modular synthetic protocol for the grafting of various cancer targeting peptides to address to tumor heterogeneity.

1.3 Immunotherapeutics

Immunotherapeutics aid the patient's immune system in detecting and killing cancer in the body.[8,9] Over time, cancer cells develop and evolve to hide from the immune system through genetic changes that lower chances of detection, expressing anti-immune proteins that down-regulate immune cells, or manipulation of the surrounding healthy tissue to interfere with immune responses.[10] Many types of immunotherapeutics have been developed to address these evasion methods and improve the immune response against cancer[11]. Examples of immunotherapies include checkpoint inhibitors, which block the regular immune checkpoints to encourage more robust immune responses; T-cell therapies, which include genetically modifying T cells to recognize cancer therapies (i.e. Chimeric Antigen Receptor T cells (CAR- T Cells), or adoptive cell therapy to select and expand strongly active T cells;[12,13] therapeutic antibodies that target to and coat the cancer and act as signals to the immune system for cell death; and finally immune modulators such as cytokine treatment or T cell Engagers[14], which act as adaptors between T cells and cancer cells, by-passing the classic T cell activation pathways (Figure 1.1) for a more robust response. In this thesis, I aim to develop a new type of T cell Engager that provides a strong and specific immune response to targeted cancers.
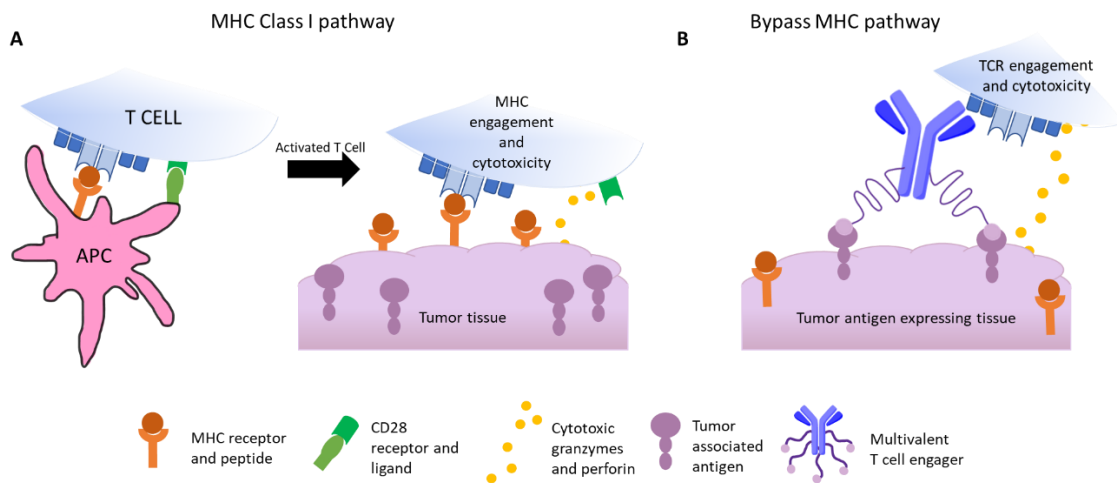
Figure 1.1 T cell engagement in traditional MHC and in bypassed pathways.
A) The T cell is presented a peptide fragment by the antigen presenting cell's (APC) MHC receptor (Orange), binding to the T Cell receptor (TCR) and the signal cascade activating the T cell is confirmed by costimulatory interaction of the APC's CD28 ligand binding to the T cell's CD28 receptor. The T cell is then ready to recognize the same peptide when presented on the cell surface of an infected cell, through their MHC receptors. However, in B) the MHC peptide presentation and second signal co-stimulation is bypassed, and the CD3 domain of the TCR is directly bound to stimulate cytotoxic pathways in the presence of the infected cell.

1.3.1 Bispecific T Cell Engagers and their limitations

The most common type of T cell engager is the Bispecific T cell Engager (BiTE)[1,4,15] and currently, there are numerous Bispecific T cell engagers in clinical trials to treat various types of cancer including, but not limited to, prostate cancer[16,17], brain cancer[18], small-lung cancer[19], and gastric cancer[20]. As well, a B-cell lymphoma BiTE, targeting the CD19 antigen (Blinatumomab), has been approved by the food and drug administration (FDA) and Health Canada[21–23]. BiTEs, made of two small single chain variable fragments (scFv; Figure 1.2), work by simultaneously binding to the cancer cell, via a tumor

4

associated antigen (TAA), and the T cell, via the CD3 domain of the T cell Receptor (TCR).

Dual binding is required to activate cytotoxic pathways in the T cells for apoptosis of the

nearby cancer cells, by-passing the classical major histocompatibility complex (MHC) and

co-stimulatory pathway of T cell activation and allows for a polyclonal T cell response,

regardless of their antigen recognition capabilities.[24,25]
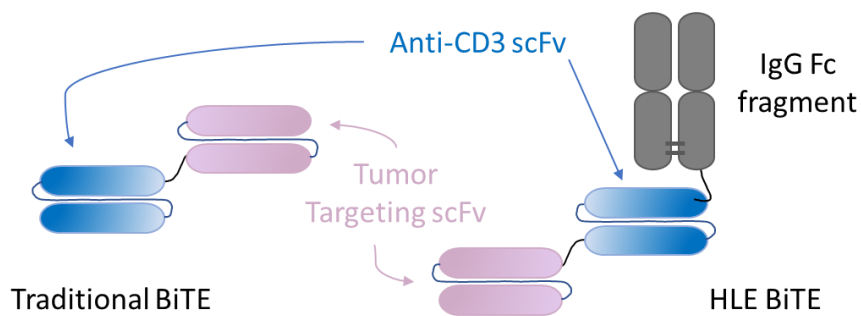
Figure 1.2 Traditional and Half-life extended (HLE) Design of BiTE.
The BiTE contains a scFv targeting to the tumor via specific tumor antigens (pink), and a
second scFv to engage the T cell (blue). The HLE-BiTE has a small Fc fragment conjugated
to the anti-CD3 scFv to increase the size and utilize Fc-mediated recycling to improve
retention within the body.

Despite the success of the BiTE to elicit a targeted and robust response, they face

several limitations such a (1) short plasma half-life (blinatumomab has ~ 2-hour half-life

in patients)[21,23], requiring continuous infusions to maintain therapeutic concentrations,

resulting in patient discomfort and long-term infusion results in risk of systemic

toxicity[26]; (2) low solid tumor efficacy[27] due to poor tumor uptake; (3) on-target off-site

cytotoxicity;[4,14] and immune escape by the loss of the BiTE targeted TAA. In the original

design of the BiTE, their small size was expected to have strong biodistribution

(movement through the blood system and tissue) and encourage tumor penetration for

better intratumoral therapy. However, clearance from plasma is much faster than their distribution to and into the tumor site; resulting in the need for continuous infusion at low doses to maintain the minimum therapeutic concentration, with the risk of systemic toxicity. Recently, the half-life-extended BiTE (HLE-BiTE, Figure 1.2) was developed and has been moving through pre-clinical assessment to address the BiTEs high clearance rate.[19,28,29] The addition of an innocuous Fc region to the small scFv BiTE encourages longer plasma half-lives through the increase in size and Fc receptor recycling. This addition allows for maintained biodistribution and improved retention in the body with less frequent dosing, however, improved solid tumor efficacy has yet to be assessed thoroughly, and systemic toxicity through cytokine release storm (CRS) cases have been reported more frequently than the traditional BiTE.[5,29]

1.3.2   Considerations for Redesign from other T cell Engagers

Since the development of the CD3xTAA BiTE designs, there have been numerous other T cell engagers designed that aim to address one or more of the BiTE's limitations. These re-designs have included increasing the number of TAA antibodies for bi-, and tri-valent cancer targeting regions,[30–33] conjugation of anti-CD3 and anti-TAA antibodies to nanoparticles and liposomes,[30,34,35] and other more complex, albeit interesting and effective, designs including pro-drugs activated only in the tumor micro-environment (TME), virus-delivered T cell engagers, and BiTE delivering CAR-T cells.[36–39]

Multivalent tumor targeting

Multivalent tumor targeting T cell engagers can be designed to improve the on-site targeting of the T cell engager to reduce the cell death of healthy low expressing cells. A HER2 targeting bivalent T cell engager that involved the addition of a second HER2 variable region on to the antibody, demonstrated the benefits of multivalent targeting. The HER2 targeting paratopes of the antibody were designed to have a lower affinity than the traditionally used HER2 antibody, creating stronger, stable binding on over-expressed HER2 cells, and less stable binding on low-expressing cells[33]. Similar bi- or tri-valent techniques have been employed by other researchers to encourage on-site targeting, indicating that multivalent platforms have a bright future in the field of immunotherapies.[40,41]

Modularity through target antibody conjugation

Nanoparticles and liposomes coated in TAA targeting and anti-CD3 engaging antibodies or BiTEs, have been developed as a method to address the plasma half-life BiTEs. Nanoparticle Multivalent T Cell Engagers (NanoMuTEs) utilize liposomes that house specific numbers of conjugated antibodies targeting CD3 and TAA.[42] These antibody decorated liposomes were shown to be modifiable to change the anti-TAA antibody to suit the cancer being targeted, with a half-life longer than the BiTE, (PEGylated nano-MuTE $t_{1/2}$ ~50 hours compared to ~2 hours for CD19 BiTE) and strong anti-tumor activity *in vivo* (BiTE was not compared in this study). The process of utilizing liposomes as delivery agents is costly and time-consuming and the half-life is still

relatively low and would require frequent dosing as well.[43] However, this construct does provide a proof of concept for modular platforms that assist in multiple cancer targeting and combating tumor immune evasion.

Proteolytic trigger for BiTEs

Finally, increasingly complex designs have been created to attempt to improve upon BiTE properties, including conditionally activated T cell engagers, such as COBRA T Cell Engagers (Conditional Bispecific Redirected Activation).[36] These, when folded correctly, create a dual scFv structure with a small albumin region for improving half-life, much like the HLE-BiTE. Unlike the BiTE, the anti-CD3 scFv is blocked by a cleavable linker, which involves the use of proteases to cleave and reveal the anti-CD3 domain. Their main improvement from the BiTE is the potential to decrease systemic T cell activation, as the linker is more likely to be cleaved in the protease rich TME region. However, they still use a strongly binding tumor antigen targeting domain which is likely to suffer from off-site targeting.[4] The drug showed significant tumor reduction in mice, but further characterization would be needed to determine if the complex fabrication is beneficial compared to the simpler HLE-BiTEs.

1.4 Local Delivery of Immunotherapies

In addition to the characteristics of the T cell engager, the method of delivery to the patient is equally important. Local delivery allows for two main benefits over intravenous injections: (1) decreased systemic toxicity, as immunogenic materials are

8

not circulating in large concentrations throughout the body, and (2) controlled administration of drugs to the tumor, allowing for maintenance of therapeutic concentrations for longer with less frequent dosing, which can improve quality of life of the patients. Local delivery, via implantation or intratumoral injection of drug loaded vehicles, has allowed for the administration of immunotherapeutics while limiting systemic toxicity. For local delivery, immunotherapeutics are typically administered through intratumoral injections or implanted into the tumor resection cavity after resection surgeries. Direct intratumoral injection of checkpoint inhibitor anti-CTLA4 and T cell modulator anti-CD40, or injection of anti-PD-1 in an alginate gel, allowed for sustained therapeutic efficacy in the local environment and remarkably reduced toxicity.[44–46] Utilizing these delivery systems in combination with other mechanisms to increase the retention of the T cell engaging construct would reduce systemic toxicity as well as improve patient comfort.[47,48] These other mechanisms, such as increase in size and PEGylation, would usually impede biodistribution of the drug throughout the body for intravenous delivery, however from a local delivery aspect these are not a concern, but a benefit.

Improved tumor killing efficacy is seen in several other IgG based or IgG-like T cell engagers.[33,49,50] For example, a PSMAxCD3 bispecific, showed that IgGsc (IgG-like) constructs were able to localize to the tumor with effective anti-tumor activity *in vivo*, whereas Fabsc (F_{AB}-like) constructs were cleared well before anti-tumor activity occurred, even with more frequent dosing than the IgGsc.[50] This further indicates that

9

the hydrodynamic size of the MuTE, and the slower clearance associated with that, will be beneficial to the anti-tumor efficacy.

1.5 MuTE Design for Locally Delivered T Cell Engager

The previously mentioned characteristics of an optimized T cell engager, with the prospects of local delivery administrations were taken into consideration in the design of the multivalent T cell engagers (MuTEs).

1.5.1 *Full antibody and EO modification for increased retention*

To improve the half-life, in an effort to reduce dosing frequency while maintaining therapeutic concentrations, the MuTE scaffold was designed to have a larger hydrodynamic radius than a traditional BiTE. Size is influenced by the full anti-CD3 antibody and modification with short ethylene oxide (EO) oligomer linkers. The short EO linkers increase size and aim to improve retention near the site of administration by slowing diffusion and reducing clearance rates.[51,52] The increased size of the MuTE compared to the BiTE may affect tissue penetration, although PEGylation has been previously shown to improve tissue penetration by slowing clearance rates,[53] even though diffusion rates are slower. Therefore, intratumoral injection of MuTEs should improve targeted tumor cell death by remaining in tumor tissue longer.[54]

1.5.2 *Simple synthesis*

To make the MuTE scaffold synthetically simple and modular, to adapt for therapies that target tumor heterogeneity, the anti-CD3 antibodies were conjugated

with heterobifunctional EO linkers with an NHS-ester on one end, and DBCO motif on the other. As shown in Figure 1.3, this creates a two-step synthesis pathway, with the NHS-ester reacting with lysine residues on the antibody for stable oligomer conjugation and the DBCO motif reacting, via strain promoted azide-alkyne cycloaddition (SPAAC), with the cancer targeting peptide (CTP) that possesses an azide. SPAAC is an efficient chemical reaction, allowing for quick and high yield conjugation of the targeting peptide to the antibody.
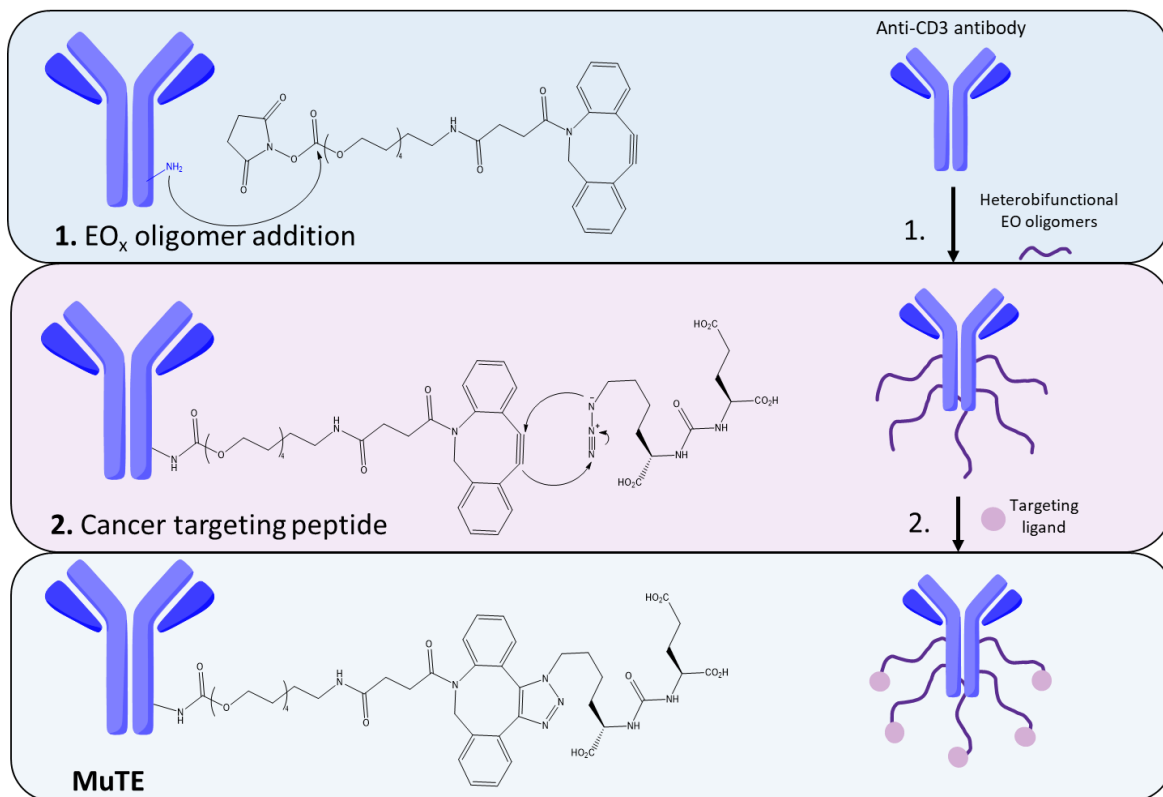
Figure 1.3 Chemical and Schematic Synthesis of MuTE utilizing an azide modified cancer targeting peptide.
Step 1) shows the conjugation of the heterobifunctional EO linkers via an NHS-ester and lysine reaction. Step 2) involved using SPAAC to conjugate the cancer targeting peptide (shown with GUL-Az) to the DBCO motif of the EO linkers, with the final MuTE structure shown in the last box.

1.5.3   Modularity for expanding to other cancer targets

In addition to SPAAC being utilized for simple synthesis, the modular platform can easily incorporate a wide range of cancer targeting peptides. Many peptides specifically targeting to a wide range of cancers already exist for various applications,[55,56] such as in cancer.[57] Therefore, with the addition of a simple azide group to any of these already existing peptides, we can take advantage of this expansive library for the MuTE

platform. When all these design aspects are brought together, the MuTE is a quickly fabricated T cell engaging construct that allows for expansion to other targets, with a broad cancer targeting peptide library.

1.6   Targets for MuTE Scaffold

The MuTE platform is designed to be easily modified with readily available cancer targeting peptides, most of which are designed for cancer diagnostic imaging. Existing CTPs already make up a large library for targeting to many different types of cancers and different targets for phenotypically different cancers.[58,59] In this thesis, we take advantage of a targeting peptide for prostate cancer (via prostate specific membrane antigen; PSMA) and human epidermal growth factor 2 (HER2) expressing breast cancer.

1.6.1   Prostate cancer

Prostate cancer is the most common type of cancer in men in the United States, and relapse is very common in treated patients. Prostate specific membrane antigen (PSMA) is a surface receptor expressed on 97% of prostate cancer patients, at many stages of progression. This makes it an exceptional targeting antigen for diagnostics and treatment. PSMA, which is a glutamate carboxypeptidase II enzyme, functions to hydrolyze *N*-Acetyl-L-aspartyl-L-glutamate (NAAG) into glutamate and *N*-acetyl aspartate. PSMA targeting is well established in both radiolabeled diagnostics and in treatment of prostate cancer by immunotherapies. PSMA is often targeted by a library of anti-PSMA clones and is also well targeted by a vast library of small molecules. These

small molecules, which have been extensively studied by for PET-tracers, are often

agonists of the by-products in NAAG hydrolysis by PSMA and act as inhibitors.[60–63]

Originally designed by Kozikowski group, urea-based inhibitors have become very

popular as small molecule based PSMA targeting ligands.[63] Specifically in this thesis,

Glutamate-Urea-Lysine (GUL; Figure 1.4) is used as the PSMA targeting ligand for the

MuTE. Of note for urea based PSMA targeting ligands, is that a spacer is required

between the targeting ligand and the "payload" (i.e., radiotracer, antibody), as the

binding site is ~20 Å deep in the PSMA extracellular domain[57]. These steric

considerations are accounted for by utilizing EO-linkers on the anti-CD3 antibody for

GUL ligand binding to the PSMA receptor. As mentioned in the MuTE design, multiple EO

linkers are conjugated to each antibody which will result in multiple low affinity binding

units to create an avidity-based targeting system.
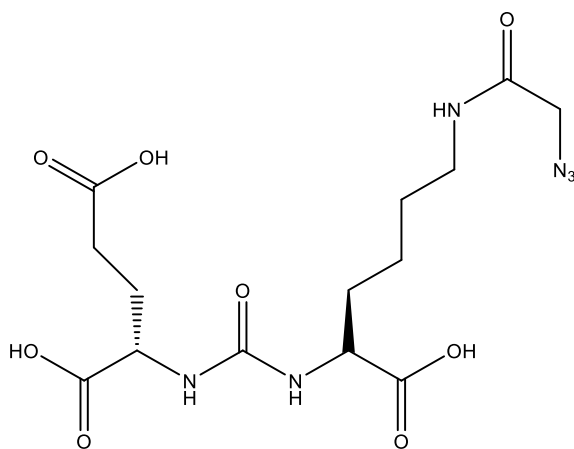
Figure 1.4 Glutamate Urea Lysine azide (GUL-Az) structure.
Figure made in ChemDraw.

In 2012, the design of the first PSMAxCD3 BiTE (pasotuxizumab) was published,

following in the footsteps of the well established Blinatumomab (CD19xCD3 BiTE),

showing its efficacy in prostate tumor regression in mice. In 2020, the PSMA BiTE

published data for its first in human dose escalation clinical trials, where the results

showed several serious adverse events, but overall, a 50% decrease in most patient's

prostate cancer burden, with 2 out of 16 patients demonstrating long term reduction.

However, before more testing was done using pasotuxizumab, the HLE PSMA BiTE

(acapatamab) was developed and in 2021 the first data was published, showing similar

preclinical efficacy as it's predecessor, and has already made its way into clinical trials. In

this thesis, we compare the efficacy and retention of the PSMA MuTE to the classic

PSMA BiTE (pasotuxizumab) in an *in vitro* 3D embedded spheroid assay to demonstrate

the longer duration of activity of the MuTE structure.

1.6.2 HER2 Cancers

To highlight the modularity of the MuTE scaffold design, the MuTE was adapted

to target human epidermal growth factor receptor 2 (HER2) expressing cells. HER2 is a

commonly used target in breast, stomach, ovarian, and many other cancer treatments,

with a common therapeutic for HER2 positive breast and stomach cancers being

trastuzumab (Herceptin), a monoclonal HER2 antibody. Currently, there is no

commercialized HER2 targeting BiTE, however there are many researchers working

toward making HER2 based T cell engagers.[30,33,64] To be consistent with the PSMA MuTE,

the HER2 MuTE follows the same structure with the targeting ligand being a 10 amino-

acid long HER2 targeting peptide (Figure 1.5).

Lys-Gln-Asp-Val-Asn-Thr-Ala-Val-Ala-Trp
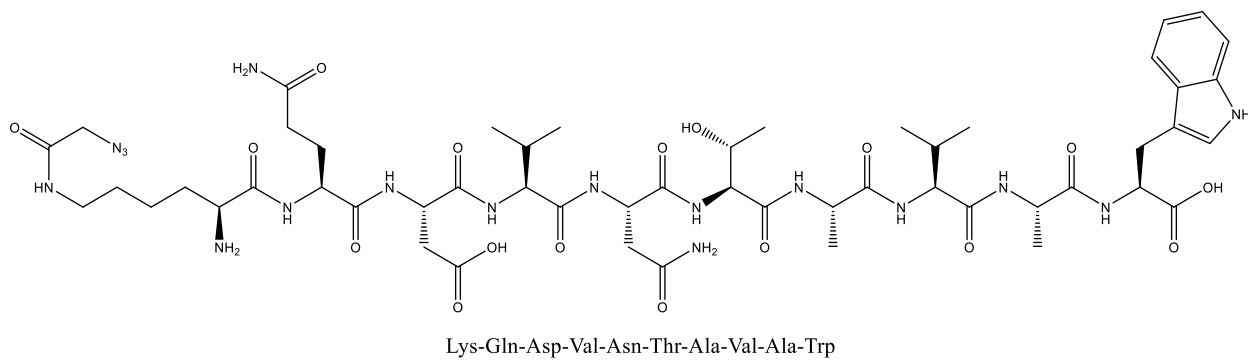
Figure 1.5 HER2 targeting peptide structure and sequence.
Figure made in ChemDraw.

Chapter 2 – Multivalent Antibody Scaffold as T Cell Engagers for Local Immunotherapies

2.1 Abstract

Immunotherapeutics that redirect the immune system toward cancerous cells have shown great promise for the development of new therapies. T cell engagers, such as BiTEs, are moving through clinical trials for many types of cancers. However, their small size and lack of recycling results in short plasma half-lives that prevents the attainment of therapeutic concentrations in solid tumors. Therefore, optimizing BiTEs for local therapies that are directly injected into the tumor offers a potential strategy to achieve therapeutic concentrations while minimizing systemic toxicity. To this end, we have developed a T cell engager with a larger scaffold to improve retention time near the site of administration. Moreover, the modular scaffold allows for the easy exchange of cancer targeting ligands towards addressing tumor heterogeneity. Using strain promoted azide/alkyne cycloaddition (SPAAC)-based conjugations, an anti-CD3 antibody was modified with short ethylene oxide $((EO)_x)$ linkers that are subsequently modified with cancer targeting peptides (CTPs). The click-based fabrication of multivalent T cell engagers (MuTEs) may address tumor heterogeneity by taking advantage of the numerous previously identified cancer targeting peptides. Ideal grafting densities for MuTEs were determined and tested *in vitro* in PSMA positive and HER2 positive cancers. In a local delivery model, using embedded PSMA expressing spheroids, MuTEs

significantly outlasted and outperformed traditional BiTEs over a 2-week period, with 2.5-fold more cytotoxicity in the MuTEs than BiTEs after 12 days.

2.2 Introduction

With the aim of overcoming transport barriers associated with solid tumors, local delivery strategies for immunotherapeutics are actively being explored and developed. For local delivery, immunotherapeutics are typically administered through intratumoral injections or implanted into the tumor resection cavity after resection surgeries to immediately achieve therapeutic concentrations. Immunotherapeutics can also be administered within vehicles to sustain local drug concentrations to minimize redosing. Additionally, local delivery reduces the risk of systemic toxicity, as immunogenic materials are not circulating in large concentrations throughout the body, allowing for the administration of a wider range of therapeutics. For example, direct intratumoral injection of checkpoint inhibitor anti-CTLA4[44] and T cell modulator anti-CD40[46], or injection of anti-PD-1 in an alginate gel,[45] allowed for sustained therapeutic efficacy in the local environment and reduced toxicity. Bispecific T cells engagers (BiTEs), which redirect the cytolytic activity of a sub-population of T cells towards cancer cells, are particularly interesting for local delivery strategies because of their short plasma half-life and resulting poor tumor uptake.

The efficacy of locally administered BiTEs will be primarily dependent on their clearance rate from tumor tissues,[5,65] which will require a reconsideration of BiTE

scaffolds that were primarily designed for intravenous (IV) administration. Small BiTE

structures composed of two linked single-chain variable fragments (scFv) that bind to

the T cell CD3 receptor and a cancer surface marker were first popularized, aiming to

improve tissue penetration and specificity. BiTEs act as a small adapter for T cell

dependent cellular cytotoxicity, through granzyme degranulation and perforin

release.[21,24] The anti-CD3 domain activates T cells bypassing the MHC pathway in the

same manner as previous T cell engagers. BiTEs continue to face limitations from their

relatively short plasma half-life, with the half-life of blinatumomab being ~2 hours.[4,21,26]

Recently, half-life extended BiTEs (HLE-BiTEs), that incorporate an Fc domain to reduce

clearance by promoting Fc recycling and increasing the hydrodynamic radius, were

developed to decrease dosing frequency.[17,19,28] The high clearance rate of BiTEs has also

be linked to poor efficacy in solid tumors,[66] therefore, BiTEs used intratumorally should

minimize clearance rates from tissue, and new T cell engaging scaffolds should be

explored to maximize efficacy.

To decrease protein clearance rates from tissue injection sites, modifications of

protein therapeutics are typically performed to reduce diffusion rates and clearance

rates. Typically, two primary methods are explored 1) increased the protein molecular

weight (MW), as with HLE-BiTEs, or 2) modification with low-fouling oligomers and

polymers to increase the hydrodynamic radius and minimize clearance and degradation

mechanisms. Even though PEGylation decreases protein diffusion rates, PEGylated-EGF

was previously shown to reduce elimination rates by an order of magnitude and

increased predicted brain tissue penetration distance two to three-fold.[53] The development of T cell engagers for local therapies can potentially take advantage of large protein structures modified with low-fouling oligomers or polymers, which also creates opportunities to simplify production protocols and increase targeting ligand diversity towards addressing tumor heterogeneity.

Herein we describe the modification of IgG anti-CD3 antibodies with cancer targeting peptides (CTPs) using monodispersed, bifunctional ethylene oxide oligomers ($(EO)_x$) linkers to synthesize Multivalent T cell Engagers (MuTEs) for applications in local delivery. The larger MW and EO modification of MuTEs will slow clearance rates from the injection site.[51,52,67,68] Previously, improved tumor killing efficacy and tumor localization has been reported for several IgG based or IgG-like T cell engagers compared to similar F_{AB} based therapies due to slower clearance rates[33,49,50]. By taking advantage of the known CTPs, primarily discovered for cancer imaging, different MuTEs can be easily developed for numerous cancer targets because of their simple fabrication protocol. Synthesis of the MuTE scaffold requires two-steps (**Figure 2.1a, S2**), in which there are three components: (1) the anti-CD3 targeting antibody, (2) NHS ester-$(EO)_x$-Dibenzocyclooctyne (DBCO) linkers, and (3) azide modified small peptide cancer targeting ligands. The core of the MuTE is the anti-CD3 antibody modified with hetero-bifunctional EO_X linkers that contain an amine reactive NHS group and an azide reactive DBCO group. The DBCO handle on the EO_x linkers allows for click addition via strain

promoted azide-alkyne cycloaddition (SPAAC) of the azide modified CTPs (**Figure S2**).

Therefore, the MuTE-like structures have promise for applications in local therapies.

Prostate cancers (PCs) represent a good first target for MuTEs as a well

characterized CTP has been identified for the homogenously expressed prostate

membrane antigen (PSMA), with 97% of patients having PSMA positive tumors[69]. Herein,

we utilize the glutamate urea lysine (GUL) CTP to target PSMA expressing LNCaP, PSMA

over-expressing HEK293 cells (HEK-PSMA) and controlled against a PSMA negative cell

line (HEPG2). Characterization and optimization of the MuTE scaffold was performed

with monolayer (2D) *in vitro* assays for T cell promoted targeted cytotoxicity (Figure 2.1).

As well, a collagen-HA embedded 3D spheroidal assay demonstrated improved efficacy

in a local delivery environment compared to the PSMA BiTE (pasotuxizumab).
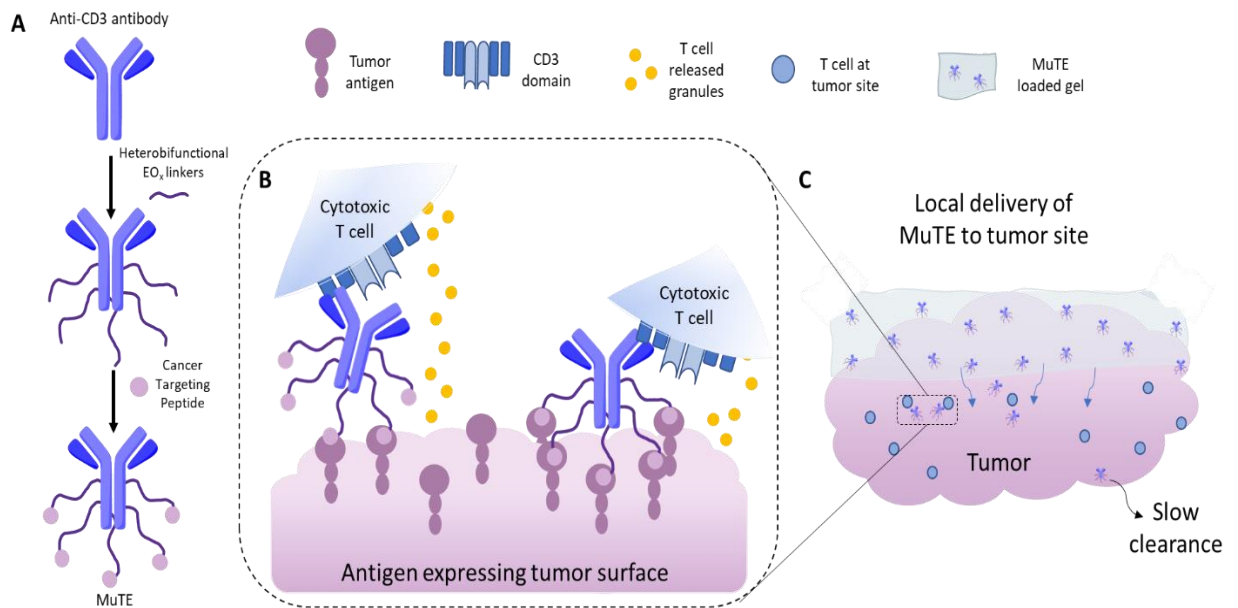
Figure 2.1 Development of Multivalent T cell Engagers (MuTEs) for local immunotherapy.

Schematic of (A) the two-step synthesis of Ligand Grafted MuTEs by heterobifunctional EOx modification of the anti-CD3 antibody and conjugation of the CTP. (B) T cell (CD3 domain) and cancer cell (tumor antigen) interactions on antigen expressing (purple) tissues. T cells release granulocytes upon dual binding of the MuTE in the presence of cancer antigens. (C) Local delivery of MuTEs to cancer cells improves efficacy due to slower clearance rates compared to traditional BiTE structures.

2.3   Materials and Methods

Materials

UCHT-1 anti-CD3 *InVivoMAb* antibody was purchased from BioXCell. OKT3 anti-CD3 antibody (Invitrogen), RPMI 1640, DMEM, and FBS were all purchased from Fisher Scientific. NHS-PEG$_4$-DBCO was purchased from Click Chemistry Tools. NHS-PEG$_{12}$-DBCO was purchased from BroadPharm. GUL-Az ((Lys(N$_3$)-glutamate-urea), HER2-Az peptide (sequence: Lys(N3)) QDVNTAVAW), PSMA BiTE, LNCaP cell line, HEK-PSMA cell line, were received from the Rullo Lab. HEPG2 cell line was received from the Zhang Lab. Raji

luciferase cells were purchased from FenicsBio. T Cell activator, IL-2, XF T-Cell media, lymphoprep density gradient, SepMate tubes, and Aggrewell800 plates were purchased from STEMCELL Technologies.

Methods

Synthesis of MuTE library

UCHT PSMA MuTEs

UCHT-1 antibody was modified with either NHS-$(EO)_4$-DBCO or NHS-$(EO)_{12}$-DBCO as follows: 100 µg of UCHT-1 antibody (6.09 mg/ml) was reacted overnight with 10, 20, or 40 eqv of NHS-PEG$_x$-DBCO linker (10 mg/ml in dry DMF) at room temperature. UCHT-$(EO)_x$-DBCO conjugates were modified with 2 eqv (relative to linkers) GUL-Az (5 mg/ml in MeOH) in PBS at pH 7.4 for 2 days at 4 °C and dialyzed against PBS at pH 7.4. Conjugation was confirmed by MALDI-TOF, and the approximate number of ligands were calculated.

OKT3 PSMA MuTEs

OKT3 antibody were modified similarly to the UCHT-$(EO)_x$-GUL with the following changes: NHS-PEG$_4$-DBCO was used in an excess of 40x, and NHS-PEG$_{12}$-DBCO an excess of 100x, and 80x and 200x ligand excess respectively. Conjugation of OKT3-$(EO)_x$-GUL were confirmed by MALDI-TOF and the number of ligands were calculated (OKT3-$(EO)_4$-GUL have 4 (EO)-GUL per antibody and OKT3-$(EO)_{12}$-GUL have 8 (EO)-GUL per antibody).

OKT3 HER2 MuTE

OKT3 anti-CD3 was modified with 100x excess NHS-PEG$_{12}$-DBCO overnight at room temperature OKT3-(EO)$_{12}$-DBCO was then modified with 200x excess HER2-Az peptide (10 mg/ml in DMSO) for 2 days at 4 °C and dialyzed (10k MWCO) against PBS. MALDI-TOF confirmed conjugation of 4-6 PEG-HER2 linkers per antibody.

Cancer cell maintenance

Prostate cancer cell line LNCaP (PSMA +, and low HER2 expression) and B cell Lymphoma cell line Raji (PSMA and HER2 negative) were maintained in RPMI 1640 media with 10% FBS. Liver carcinoma cell line Hep-G2 (PSMA negative and HER2 positive[70]) were maintained in DMEM media with 10% FBS. HEK293 cell line overexpressing PSMA (HEK-PSMA; PSMA ++, and HER2 negative) were maintained in DMEM media with 10% FBS and 50 μg/ml zeocin. SKBR3 cells (HER2 overexpressing) were maintained in McCoys 5A medium with 10% FBS. All cell lines were kept at 37 °C with 5% CO_2 and adherent cells were passaged with Tryplee disassociation reagent.

PBMC Isolation and T cell Expansion

PBMCs were isolated from fresh whole blood (<4 hours old) via SepMate tubes and LymphoPrep density gradient media following the recommended StemCell procedure. Briefly: 15 mL density media is added to the bottom of the SepMate 50 mL tube, 16 mL of whole blood is diluted with 16 mL PBS + 2% FBS and carefully layered on top of the density media. The tubes are centrifuged at 1200 g for 10 minutes and the top layer is carefully poured off and washed with PBS + 2% FBS twice (centrifuging 300 g for 8

minutes). PBMCs are counted and frozen at 5 M/mL in RPMI 1640 + 10% FBS + 10% DMSO.

T cells are expanded from PBMC frozen stocks as recommended by StemCell, briefly: PBMCs are thawed and then washed with 5 mL XFT Media with IL-2 and centrifuged at 300 g for 10 minutes. The cells are resuspended, counted, and diluted to 1 M/mL with XFT Media supplemented with IL-2 and T cell activator (25 µL per 1 mL of cell suspension). Cell suspension is plated in a 96 well round bottom plate and incubated for 3 days at 37 °C with 5% CO_2. On Day 3 the cells are diluted 8-fold in fresh XFT media with IL-2 and plated in a 24 well flat bottom plate and incubated for 2 days. On Day 5 and 7 the cells are diluted 4-fold in XFT media with IL-2 in a 24 well plate and incubated. On Day 10 or 11 the cells are harvested.

Cytotoxicity assay

E:T Ratio

In a 96 well plate, 20 000 cancer cells were co-cultured, in RPMI 1640 with 10% FBS, with the corresponding amount of effector cells (T cells; 0:1, 1:1, 3:1, or 5:1 E:T ratio) in the presence of PSMA MuTEs, PSMA BiTE, or relevant controls (final concentration 1 nM) for 24 hours at 37 °C with 5% CO_2. Luciferin was added and the luminescence was read immediately, and at 5 and 15 minutes on a Biotek Cytation 5 plate reader.

Dose Response

The MuTE or PSMA BiTE were serially diluted from 10 nM to 0.6 pM in PBS into triplicate wells of a 96 well plate. 20 000 cancer cells and 100 000 T cells (E:T ratio of 5:1) were

plated in RPMI 1640 + 10% FBS media and incubated for 24 hours at 37 °C with 5% CO_2.

Luciferin was added and the luminescence was read immediately and at 5 and 15

minutes on a Biotek Cytation 5 plate reader.

Spheroid Assay

Spheroids were prepared in Aggrewell^{TM} 800 plates following Stemcell protocol. Briefly:

HEK-PSMA cells expressing iRFP were plated at 600 000 cells per microwell (2000 cells

per spheroid) and incubated for 24 hours at 37 °C with 5% CO_2, after which they were

harvested and embedded in a collagen-HA (1 wt%) gel (5 spheroids per 10 µL) and

plated into a 384 well plate. In the same gel, 20 000 T cells and 1 nM drug (UCHT-$(EO)_{12}$-

GUL or OKT3-$(EO)_{12}$-GUL or PSMA BiTE) were added. In the No T cells control, PBS was

added in place of the T cell volume. Similarly in the No Drug control, PBS was used in

place of the MuTE or BiTE. Gels were incubated at 37 °C with 5% CO_2 for 30 minutes to

allow for gelation. 80 µL of Fluorobrite media with 10% FBS was added on top of the gel

and the media was changed daily afterward. Fluorescent microscopy images were taken

using a Biotek Cytation 5 Imager and analyzed using ImageJ.

2.4   Results and Discussion

2.4.1   *Optimization of PEGylation and linker length*

Although the use of an anti-CD3 IgG decreases clearance rate compared to ScFv

BiTEs, we first identified antibody-polymer constructs that decreased non-specific

cytotoxic activity that is commonly observed with bivalent anti-CD3 constructs. The

effect of EO_x and polymer modifications on the non-specific activity of T cells against PSMA +ve LNCaP and PSMA -ve HEPG2 cells was quantified by constructing MuTEs with 6-Azidohexanoic acid (non-targeting azide molecule) instead of the CTP. Interestingly, modification of two different anti-CD3 clones, UCHT-1 and OKT3, with an $(EO)_4$ average grafting density ~4 decreased non-specific activity (**Figure 2.2**) unlike high MW low-fouling polymers (**Figure S1**). Unmodified anti-CD3 antibodies produced a strong non-specific activation of the T cells resulting in non-specific cancer cell death, with 10% more cytotoxicity seen in the UCHT-1 clone than the OKT3 clone. Toxicity was greatly reduced upon $(EO)_x$ modification (**Figure 2.2**) with cell viability for both LNCaP and HEPG2 at ~88-90% for UCHT-1 and 105-108% for OKT3 with 1 nM doses after 24 hours. The reduced toxicity may be partially due to $(EO)_x$ shielding and reduced binding affinity to T cell CD3 domains[71], although no reduced toxicity was observed upon the conjugation of higher MW low-fouling polymers (**Figure S1**), indicating polymer properties and MW must be carefully selected.

Given the potential for greater T cell activity for local intratumoral therapies with the UCHT-1 anti-CD3 antibody, this clone was further characterized for MuTE development. UCHT-1 has greater local T cell proliferation potential than OKT3 to enhance anti-cancer activities, which may also help explain the observed differences in cell viability. It has previously been shown that immobilized OKT3 is not able to induce T cell proliferation without the presence of costimulatory cytokines (e.g IL-2), despite having a higher CD3

binding affinity (~0.5 nM) than UCHT-1 (~2 nM),[72,73] whereas immobilized UCHT-1

induced proliferation independently.[74]

A   **B**

LNCaP (PSMA +ve)   HEPG2 (PSMA -ve)
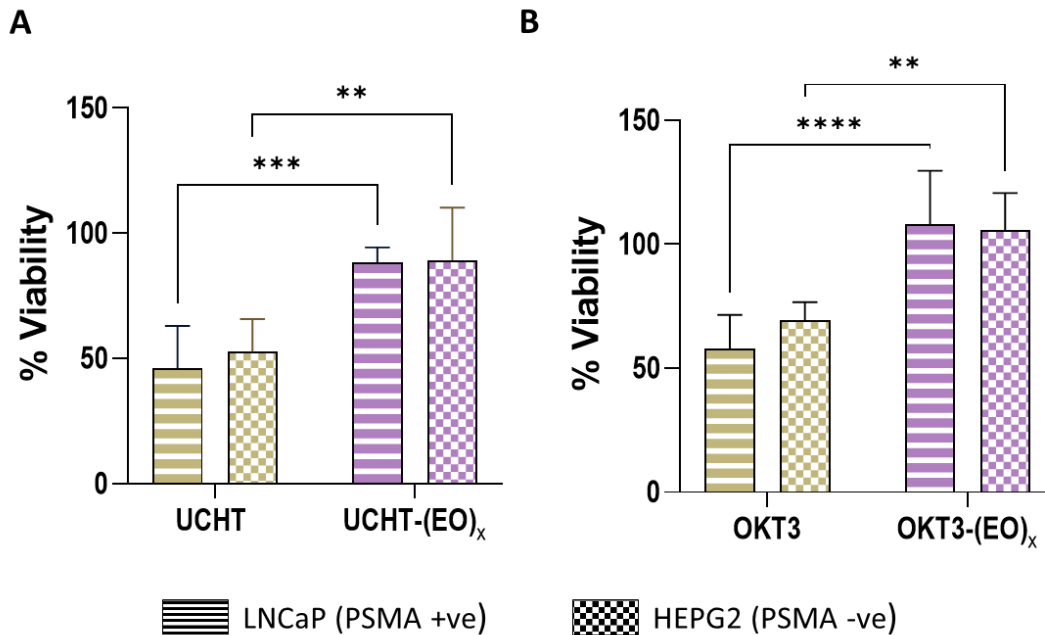
Figure 2.2 Modification of anti-CD3 antibodies with (EO)x linkers reduced non-specific cytotoxicity in co-cultures.

Unmodified and (EO)4 modified (4 linkers per antibody) A) UCHT-1 and B) OKT3 anti-CD3 (1 nM) incubated in the presence of T Cells and LNCaP and HepG2 cancer cells at a 5:1 E:T ratio; n=6, mean ± SD. Because no CTP was conjugated (DBCO is reacted with non-targeting 6-azidohexanoic acid), decreases in viability is attributed to non-specific cytotoxicity.

Upon the addition of sufficient $(EO)_x$ linkers and GUL peptides, T cell cytotoxicity

is re-established towards the PSMA expressing cell line, LNCaP (**Figure 2.3**). MuTEs with

different $(EO)_x$ linker MWs and average grafting densities on UCHT-1 antibodies were

studied. MuTEs with lower average grafting densities of $(EO)_x$-GUL resulted in non-

specific killing and no detectable targeted killing of PSMA+ LNCaP cells. At higher

grafting densities of 3-4 and 6-8 for $(EO)_4$-GUL and $(EO)_{12}$-GUL, respectively, MuTEs regained targeted killing of LNCaPs over PSMA- HEPG2s. Interestingly, $(EO)_{12}$ requires a greater average grafting density than $(EO)_4$ to minimize non-specific killing and observe specific killing; non-specific killing data without GUL in Figure 2.2 was performed with $(EO)_4$ and aligns with the data in Figure 2.3. Therefore, if different $(EO)_x$ MWs are investigated, the grafting density must first be optimized due to differences in T cell activities upon exposure to MuTEs with varying $(EO)_x$ MWs.

To determine the optimal $(EO)_x$/CTP grafting density described above, the UCHT-1 anti-CD3 antibody was modified at 3 densities with $(EO)_4$-DBCO and $(EO)_{12}$-DBCO linkers and further reacted quantitatively with an azide modified GUL (GUL-Az) CTP to create MuTEs with grafting densities of 1-2, 3-4, and 6-8 $(EO)_x$-GUL (**Figure 2.3a,b**). These constructs were then tested *in vitro* for non-specific cytotoxicity in the PSMA negative cell line, HEPG2, and compared to the targeted cytotoxicity in the PSMA positive cell line, LNCaP. Increasing the number of $(EO)_x$-GUL units per antibody reduces the non-specific activity of T cell activation, with the 3-4 units of $(EO)_4$-GUL and 6-8 units of $(EO)_{12}$-GUL MuTEs having the highest survival rate in the HEPG2 cell line (80-90% viability), while maintaining effective cell death in the LNCaPs (~50% viability). As the $(EO)_x$ linker length is increased, a greater grafting density per antibody is required to reduce the non-specific toxicity of the anti-CD3 antibody; the anti-CD3 modified with 3-4 $(EO)_{12}$-GUL was 20% more cytotoxic against PSMA- HEPG2 cells than the 3-4 $(EO)_4$-GUL unit anti-CD3.

To determine if higher $(EO)_x$ grafting densities result in loss of bioactivity due to sterics, we modified anti-CD3s with an average grafting density of 22 $(EO)_{12}$-GUL units. The 22 $(EO)_{12}$-GUL MuTEs did not promote any nonspecific or targeted T cell mediated killing of LNCaPs or HEPG2s (**Figure S3**), indicating the anti-CD3 domain is not active after the grafting ~22 $(EO)_{12}$-GUL ligands. To confirm that the lack of targeted killing was not due to poor PSMA binding, we performed a label-free detection assay for MuTE binding to a PSMA modified surface using local surface plasmon resonance (LSPR).[75] Strong association without any detectable dissociation for the MuTE-PSMA interaction, indicating that the MuTE can bind surface PSMA receptors (Table S1). The $(EO)_x$ grafting density must therefore be sufficient to minimize nonspecific killing but within a range that retains the ability to engage T cells. In this study, we determined that four $(EO)_4$-GUL or eight $(EO)_{12}$-GUL units results in targeted cytotoxicity towards PSMA positive cell lines.

Additionally, the impact of a different anti-CD3 clone used in the MuTE platform was compared. As previously mentioned, both antibodies produce similar strong non-specific cytotoxic T cell activation that can be reduced upon conjugation of $(EO)_x$. The OKT3 MuTEs were modified to have a similar grafting density to the most effective UCHT MuTEs, with four $(EO)_4$-GUL and eight $(EO)_{12}$-GUL per antibody. Between the two anti-CD3 $(EO)_4$-GUL MuTEs (**Figure 2.3c**), the UCHT-$(EO)_4$-GUL is 1.6x more effective in the LNCaPs than the OKT3-$(EO)_4$-GUL. In the $(EO)_{12}$-GUL MuTEs, there is 1.5x more LNCaP cytotoxicity in the OKT3 MuTE compared to the UCHT MuTE, with the same viability in

the HEPG2 cells (~95%). Here, the difference in binding affinity between the two anti-CD3 antibodies and the CD3 domain does not seem to significantly alter the T cell dependent cytotoxic effects of the MuTE.
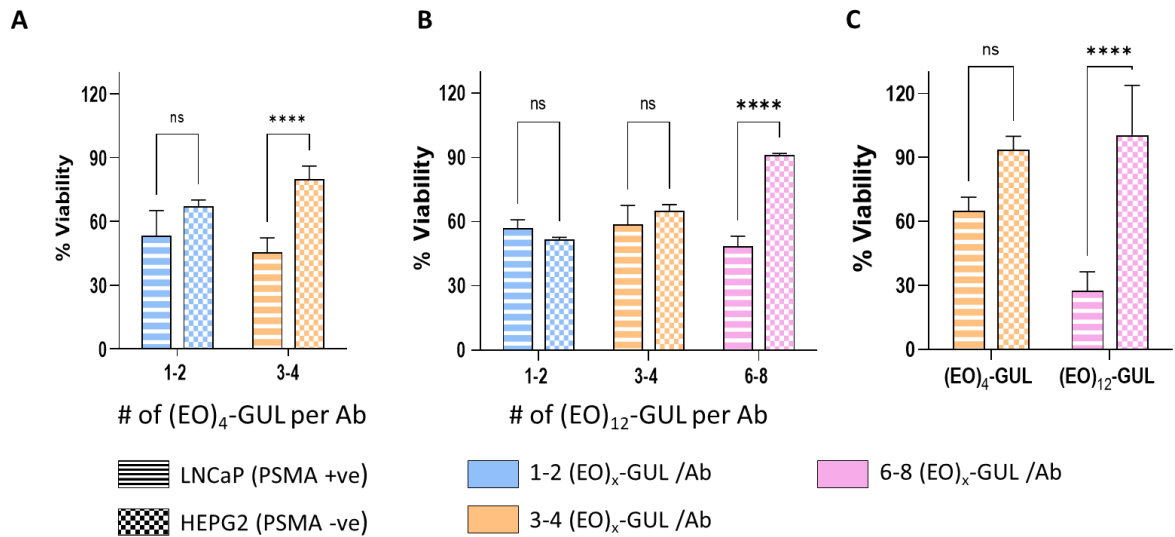
Figure 2.3 Determination of (EO)x-GUL modifications per antibody required to reduce non-specific toxicity at two (EO)x linker lengths.
A & B) UCHT-1 and C) OKT3 anti-CD3 were modified with GUL targeting ligands via two (EO)x linker lengths: A) UCHT-(EO)4-GUL (MuTE precipitation occurs at higher grafting densities, 6-8 for (EO)4 was therefore not included) and B) UCHT-(EO)12-GUL. Cancer cells were incubated with T cells at a 5:1 E:T ratio, in the presence of 1 nM drug, for 24 hours incubation (n=3, mean ± SD).

Short $(EO)_x$ linkers were chosen to achieve a distance between T cells and cancer cells similar to those observed in interactions between the TCR and target cell membrane (15 nm)[76], as well as to mimic the traditional ScFv BiTE structures, estimated to be span 12 – 14 nm between the cells.[77] The linker grafted MuTE constructs are in a maximum range of 12-16 nm in length, where an average full antibody is approximately

10 nm long[78], and the $(EO)_{4-12}$ linkers range in a contour length of 2-6 nm.[79] A small

library of MuTEs with GUL modified polymers (Figure S1B-E), in place of the short $(EO)_x$

linkers, were used to further assess the importance chain length in MuTE synthesis.

Poly(carboxybetaine-GUL) and POEGMA-GUL MuTEs (14 and 30 kDa, respectively),

copolymers with 5-10 mol% GUL modified repeat units (**Figure S1**), were unable to

reduce the non-specific killing by T cells and any potential targeted cytotoxicity was

confounded. The lack of specific killing with other polymers for CTP grafting further

demonstrates the importance for the optimization of linkers MWs.

2.4.2   Importance of PEG linker length

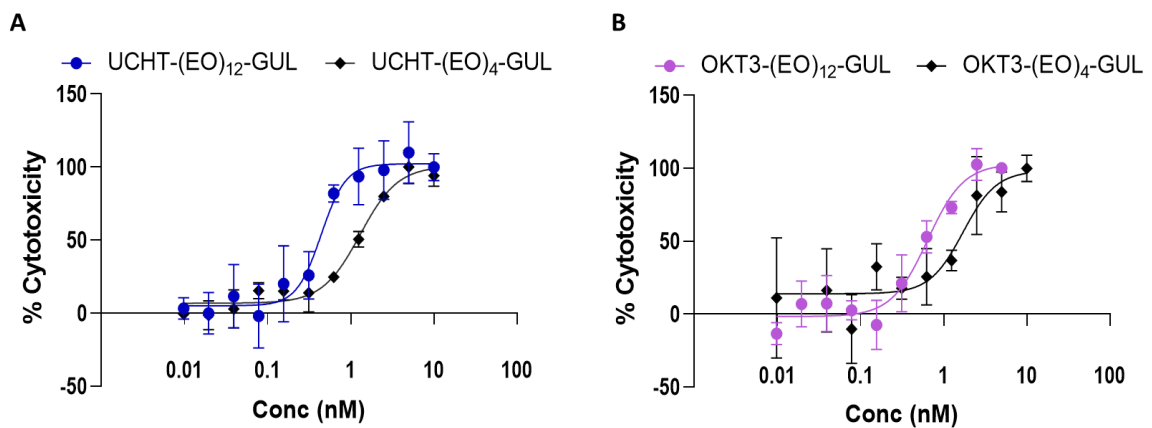**Figure 2.4 Comparison of targeted cytotoxicity at two linker lengths utilizing two anti-CD3 clones.**

Impact of PEG length on cell viability in LNCaP (PSMA positive) across many dosages was assessed at 5:1 E:T ratio, and luminescence was read after 24 hours incubation with each MuTE. Comparison of (EO)4-GUL (3-4/Ab) and (EO)12-GUL (6-8/Ab) on A) UCHT-1 and B) OKT3 anti-CD3 clones. n=3-4 mean ± SEM.

To further compare the effect of the linker length in the MuTE scaffold, a screening of dose response across 10 pM to 10 nM was performed against the LNCaP cells. When the linker length is increased, the EC_{50} value shifts lower (**Figure 2.4**). With the UCHT-1 anti-CD3, the $(EO)_4$-GUL MuTE has an EC_{50} of 1.29 nM and the $(EO)_{12}$-GUL is ~2.5-fold lower at 0.44 nM. A similar trend with the OKT3 anti-CD3 is seen, where the EC_{50} are 1.7 and 0.76 nM for the $(EO)_4$-GUL and $(EO)_{12}$-GUL respectively, yielding a ~2-fold decrease. The longer $(EO)_{12}$ vs $(EO)_4$ linker may allow for increased PSMA binding, increasing spacer size has been previously reported to aid in cell interactions with immobilized targeting peptides. Overall, the UCHT-1 and OKT3 $(EO)_{12}$-GUL MuTEs are the most effective and further *in vitro* characterization was performed.

2.4.3   *Demonstrating the modularity of the MuTE Platform*

Development of cancer targeting immunotherapeutics require months of antibody design and production to ensure accurate binding, folding, scale of production, and the more difficult task of maintaining serum stability, for every cancer target desired[80,81]. With the MuTE platform switching targets is streamlined as the base of the construct (EO linker grafted antibody) is the same for each target, and the antibody can be easily and stably produced. The addition of the tumor targeting peptide is facilitated by click chemistry, making it reliable and efficient.[82] With this platform the MuTE is synthesized and tested within a few days. To demonstrate this modularity in the platform, a small HER2 peptide was conjugated to OKT3-$(EO)_{12}$ MuTE (HER2 MuTE) and was tested against HER2 positive cell lines (**Figure 2.5**).
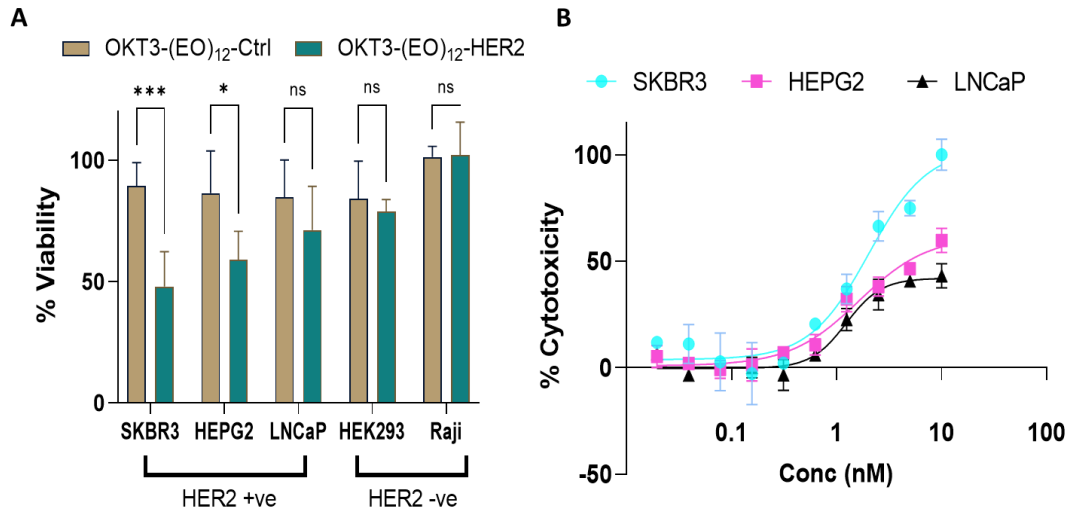
Figure 2.5 HER2 targeting MuTE demonstrates the modularity of the MuTE platform.
OKT3-PEG12-DBCO was modified with a HER2 targeting peptide and assessed in vitro. A)
Viability of various HER2 expressing or non-expressing cell lines in the presence of 1 nM
HER2 MuTE at a 5:1 E:T T cell ratio, n=3, mean ± SD, B) Dose response curves of HER2
positive cell lines at a 3:1 E:T ratio, n=3-4, mean ± SD, normalized relative to SKBR-3.

In Figure 2.5a, the HER2 MuTE shows consistent results with the PSMA MuTEs.

There is little to no non-specific T cell cytotoxicity in the non-expressing cell lines

(HEK293 and Raji) or in the non-targeting control (azido-hexanoic acid in place of the

CTP). Interestingly, as the relative level of HER2 expression increases, there is more T cell

induced cell death (**Figure 2.5**); SKBR-3s over-expressing HER2 protein by three-fold

compared to the HEPG2 and LNCaPs[83]. HEPG2s have ~40% greater expression level than

LNCaP cells (SKBR3>>HEPG2>LNCaP).[84] Although the EC_{50} values are all within a similar

range (1.2-1.9 nM), the comparative amount of cell death at higher doses decreases in

the lower expression cell lines (**Figure 2.5b**), indicating the MuTE platform does not

target cells with lower HER2 expression within the HEPG2 and LnCAP experiments. In

future iterations of the MuTE, this could further assist with reducing off-site on-target

cytotoxicity, depending on the dose and/or affinity of the individual targeting peptide.

Overall, the HER2 MuTE shows the validity of the modularity in the MuTE platform to

generate consistent results in reduced non-specificity and strong targeted cytotoxicity.

2.4.4   Increased retention and high efficacy of MuTEs in local delivery 3D model

        To compare the efficacy of MuTEs compared to traditional BiTEs in local

therapies, we developed a 3D embedded spheroid model and tracked spheroid growth

and killing over time with a single therapeutic administration. Cancer spheroids of ~200

μm were embedded within collagen-HA gels, to mimic the ECM, that also contained T

cells and either a MuTE structure or a ScFv based BiTE (**Figures 2.6a, S5**). Daily media

changes were performed to simulate clearance. iRFP expressing HEK-PSMA cells were

chosen as they readily form spheroids with a moderate and linear growth rate[85] and the

PSMA targeting MuTE and BiTE constructs are active against the HEK-PSMA cell line

(Figure S4). Spheroids were imaged over the course of two weeks via brightfield and Cy5

fluorescence microscopy (**Figure 2.6d, S5**), and the corrected total spheroid fluorescence

(CTSF) was measured via 3D z-stacks. The corrected total spheroid fluorescence (CTSF)

was measured by summing the background corrected fluorescence of image slices

across the full volume of the spheroid, and then the average spheroid fluorescent signal

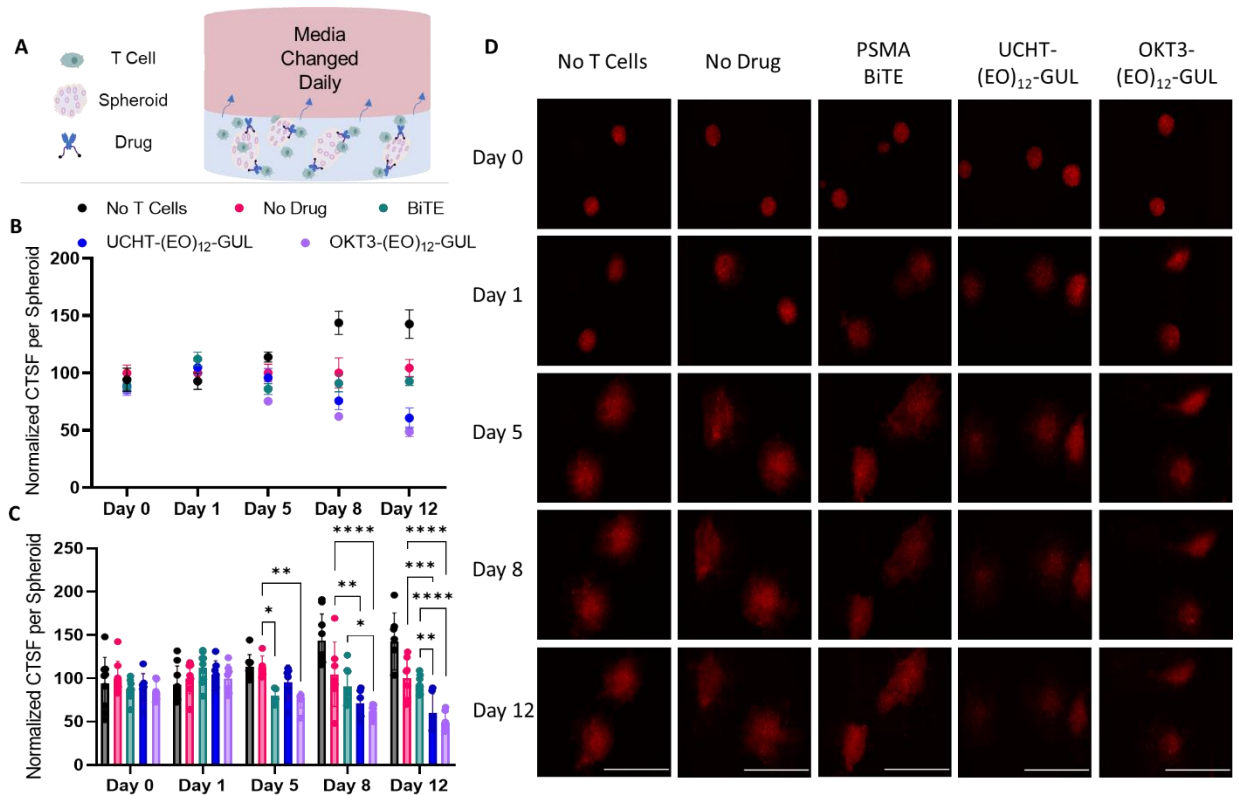per well was normalized to the no drug control wells at each timepoint.

Figure 2.6 Assessment of Cytotoxicity in Multicellular Spheroid 3D in vitro assay.
iRFP expressing HEK-PSMA spheroids and T cells embedded in a collagen-HA gel containing the MuTE or BiTE at 1 nM, or No Drug with and without T Cells. A) Schematic of the spheroids and T Cells in a well of a 384 well plate. B) Normalized fluorescent spheroid signals as a scatter plot to show trends over time, n=6-9 ± SEM. C) Average corrected total spheroid fluorescent signal per spheroid (sum of signal of z-stack encompassing entire spheroid), normalized to the No Drug signal each day, n=6-9, ± SD. Statistical analysis is done using 2-way Anova with a Tukey post-hoc test. D) Representative fluorescent (Cy5) images of spheroids in each condition over time, scale bar is 1000 μm.

Over the 12 day embedded spheroid study, both the UCHT and OKT3 MuTE

constructs sustained HEK-PSMA killing (**Figure 2.6b,c**) longer than the BiTE. From day 1

to day 12, the majority of the BiTE treated spheroid cell death occurred by day 5

(decreased 23%, from day 1 to day 5) and cell growth occurred after day 5 (7% increase

from day 5 to day 12), which resulted in a total signal reduction of 18% after 12 days.

After 5 days, the BiTE concentration was likely below the minimum effective therapeutic

concentration, most likely due to BiTE clearance from the ECM mimic. MuTE treated

spheroids monotonically decreased fluorescence from day 1 to day 12. On day 5, the

BiTE is slightly more effective than the UCHT MuTE (10% difference in fluorescence

intensity) but the OKT3 MuTE is more effective than the BiTE (12.7% difference in

fluorescence intensity). By day 8, the UCHT MuTE resulted in greater cell killing than the

BiTE, and the OKT3 MuTE maintained a steady increase in cell death. On day 12, the

fluorescent signal from the cancer spheroid decreased by 42% compared to day 1 for the

UCHT MuTE, and 51% for the OKT3 MuTE. Compared to the BiTE, the reduction in

spheroid fluorescence from the OKT3 MuTE was 2.5-fold lower, indicating greater cell

killing. Although in a 2D co-culture experiments without an ECM, the BiTE is more

efficacious than the MuTE (**Figure S4**), the 3D embedded spheroid model shows that

both MuTEs demonstrate greater efficacy for local administration protocols, suggesting

an appreciable increase in local retention and the maintenance of therapeutic

concentration.

We have therefore developed a modular synthetic platform for the click-based

conjugation of CTPs to facilitate T cell engager development for local therapies and the

targeting of immune escape and tumor heterogeneity by utilizing the existing library of

CTPs described in the literature.

Chapter 3 – Further Discussion

The future of cancer therapies should be personalized treatments for each patient, rather than just general organ or tissue type affected. The development of the MuTE platform discussed in this thesis creates a more accessibly fabricated immunotherapeutic that in the future can be personalized to the patient's specific tumor antigen expression. Ideally, an available library of radio- or fluorescent-labelled cancer targeting peptides allows for patient's tumors to be imaged for diagnosis and the same peptide would then be utilized in the MuTE platform. This would ensure effective targeting to the patient's cancerous cells to allow for strong immune responses via the MuTE. However, there are further steps for standardizing the MuTE platform that should be undertaken first.

To standardize the grafting of the linkers in the MuTE platform, site selective modification could be utilized. Currently, the antibody grafting density and location is dependent on the available lysine residues, creating potential issues for translation into the clinic. However, fabricating an anti-cD3 antibody with unnatural amino acids at locations outside of the variable/paratope region, would allow for linker addition through unique chemical conjugation at specific locations.[86,87] This has been demonstrated in a modified version of trastuzumab, incorporation of an unnatural amino acid and conjugation of a small drug molecule via oxime conjugation, improved the pharmacokinetics over cysteine conjugation.[88] Alternatively, utilizing the

glycosylation of the Fc region for enzymatic site-specific conjugation could also be explored.[87] Modifications of glycotransferases can allow for the addition of monosaccharides containing unique reactive handles can be incorporated onto the antibody.[89] Enzymatic modification offers the benefit of avoiding engineering (as required for unnatural amino acids), however, enzymatic conjugations are known to create heterogenous antibody drug conjugates, potentially creating unique problems, as well as limited modification sites.[90] Further exploration of site selectivity to ensure standardized antibody modification could be beneficial to future iterations of the MuTE platform.

Chapter 4 – Conclusion

T cell engagers with slower clearance rates for applications in local immunotherapies have the potential to improve efficacy against solid tumors. MuTEs showed promise for increased retention and maintenance of therapeutic levels within the 3D local delivery model against PSMA expressing spheroids by outperforming cytotoxicity of BiTEs by 2.5-fold, indicating the MuTE scaffold may be useful for the local treatment of solid tumors. In addition to this, the MuTE scaffold can be easily expanded to virtually any targetable cancer with peptides, as demonstrated with PSMA and HER2 expressing cancers. The modular MuTE platform is not limited to homogenous CTP conjugations, MuTEs can be modified with heterogenic CTPs to overcome tumor immune evasion and increase specificity.

Chapter 5 – Future Directions of MuTE Platform

5.1 Heterogeneous Cancer targeting

Moving beyond the single targeting antigen on the MuTE scaffold to have two or more tumor targeting antigens conjugated to the anti-CD3 antibody (Figure 5.1).
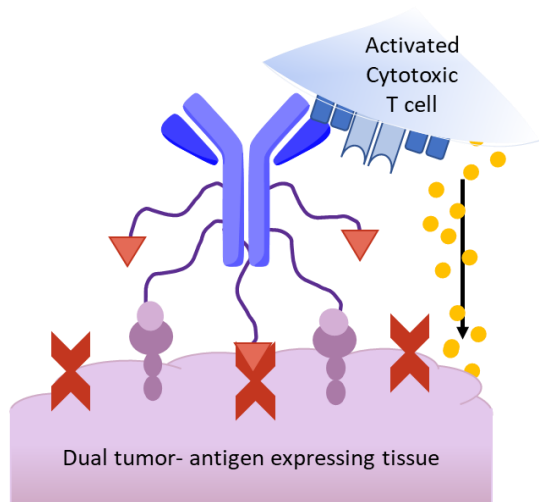
Figure 5.1 Multi-antigen MuTE engagement.
Two distinct cancer targeting peptides (Red triangles, purple circles) are bound to their respective tumor antigens, and the anti-CD3 antibody is engaging and stimulating the T cell to release cytotoxic granules (yellow circles).

5.1.1 Benefits of multi-antigen targeting

Like healthy cells, cancerous cells express many receptors and proteins on the surface of the cell, however, these are usually erroneously over-expressed. Many cancers are not homogenous in the over-expression of tissue specific antigens and are similar in receptor expression to their healthy tissue counterparts. Targeting these cancers is more difficult as the risk of targeting to healthy tissues is higher. Targeting to

more than one of the receptors that is over-expressed on tumors would allow for improved targeting specificity and reduce off-site T cell activation. Additionally, utilizing heterogenic targeting could potentially allow for multiple types of cancers to be targeted at once, allowing for personalized, unified treatment for patients.

5.1.2   *Potential synthesis of multi-antigen MuTEs*

To synthesize these multi-antigen T cell engagers would maintain the fundamental basics of the MuTE scaffold already developed here. A potential synthesis pathway and the benefits and limitations will be briefly described (Figure 5.2):

Two-Stage DBCO-Azide

Method:

The anti-CD3 antibody would be modified with half the necessary number of NHS-EO_{12}-DBCO linkers (3-4/Ab) and reacted with targeting ligand A, creating anti-CD3-EO_A. Next, the anti-CD3-EO_A would be modified with additional NHS-EO_{12}-DBCO linkers, to bring the total to 6-8 EO_{12} linkers per antibody, and modified with targeting ligand B, creating a PEGylated anti-CD3 antibody with two unique targeting ligands.
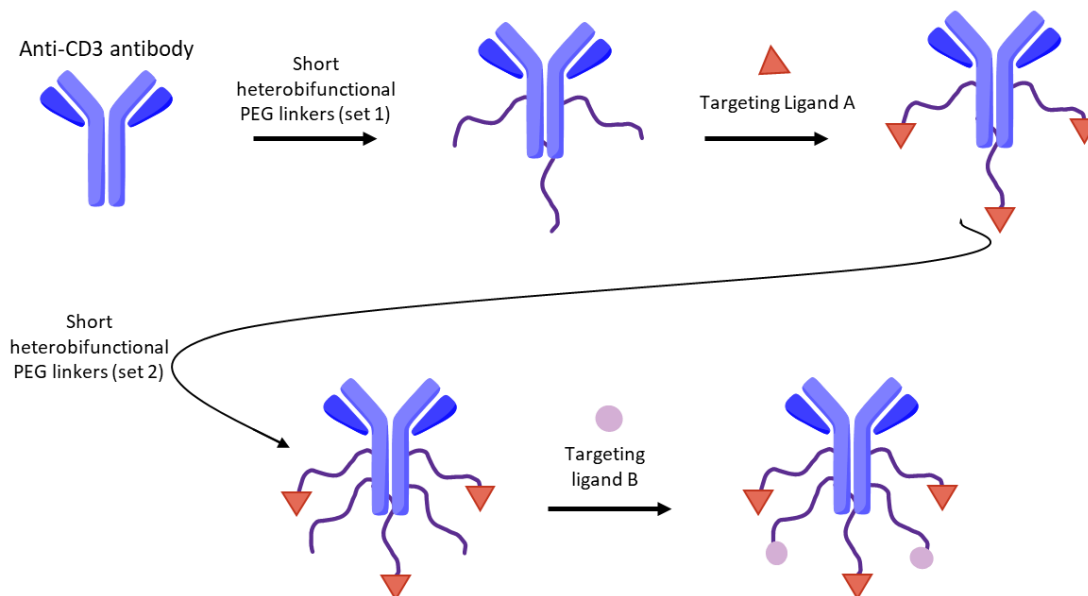
Figure 5.2 Synthesis of Multi-antigen MuTEs.
Initial set 1 EO_x linkers are conjugated to the anti-CD3 antibody and reacted with Ligand A (red triangles). Then, additional EO_x linkers (set 2) are added to the modified antibody and conjugated to Ligand B (purple circles).

Benefits and limitations

This method retains the same chemistry that has been described and optimized here, allowing for a library of azide-linked peptides to be utilized in numerous combinations. However, the limitation for this method comes in the addition of the second set of EO linkers, specifically due to the NHS ester Lysine reaction. Lysine residues present in the targeting ligand A have the risk of the EO linkers being conjugated, this would limit Target A to being a peptide sequence that does not possess lysine or primary amine functional groups. Additionally, the peptide sequence would require acetylation of the N-terminal amine end to prevent cross-linking of the primary amine.

5.2 Co-stimulatory T cell activation

Development of a T cell engager that enhances the effects of the anti-CD3 T cell activation, through co-stimulatory engagement of the T cell CD28 receptor.

5.2.1 Co-stimulatory MuTE Design

The anti-CD3 x anti-CD28 x TAA MuTE would maintain the same functional set-up as the original MuTEs, with the use of a bispecific antibody in place of the mono specific anti-CD3 antibody (Figure 5.3). The cancer targeting EO linkers would continue to maintain the activation of the T cells only in the presence of the tumor antigens.
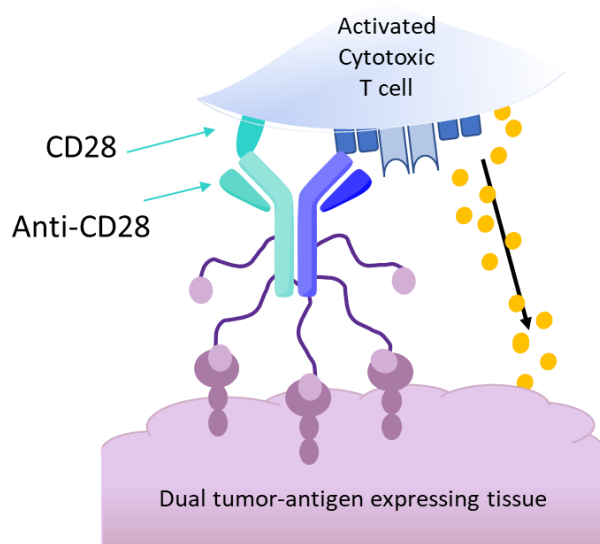

Figure 5.3 Co-stimulatory MuTE interactions.
A bispecific anti-CD3 (blue) and anti-CD28 (teal) IgG anti-body are modified with CTP conjugated EO_x linkers and interact with the cancer cell and T cell simultaneously to achieve targeted cytotoxicity.

5.2.2 Benefits of Co-stimulatory T cell engagers

The traditional activation pathway of T cells is through a two-signal mechanism, where Signal 1 is the binding of the TCR (CD3), and Signal 2 is binding to the CD28 protein. Binding of the TCR to the target cell's complementary antigen peptide presented in the MHC pocket, creates the immune synapse that activates the T cell and initiates the cytotoxic pathways and T cell proliferation. When Signal 2 is applied in the MHC pathway, either by an antigen presenting cell or by the target cell, T cell activation and proliferation are further amplified creating a more robust cytotoxic attack.[91]

In current T cell engagers, the MHC path is bypassed, and activation is facilitated by the drug acting as an adapter in place of the MHC-peptide. In the presence of the T cell engager, the T cell can recognize the cancer cell regardless of both its own TCR specificity and the antigen presented in the cancer cell's MHC domain. Most current T cell engagers do not utilize the co-stimulatory engagement; however, a few have been in development recently.[31,49,92] These dual T cell engaging constructs have shown that the use of both CD3 and CD28 engagement provide a more effective response *in vitro* and *in vivo*. Additionally, these treatments would benefit patients that are less responsive to anti-CD3 stimulation alone[93,94], as shown in several co-stimulatory T cell engaging and CAR-T therapies.[94–97]

References

(1)   Huehls, A. M.; Coupet, T. A.; Sentman, C. L. Bispecific T-Cell Engagers for Cancer Immunotherapy. *Immunology and Cell Biology*. Nature Publishing Group March 19, 2015, pp 290–296. https://doi.org/10.1038/icb.2014.93.

(2)   Hawkins, E. R.; D'souza, R. R.; Klampatsa, A. Armored CAR T-Cells: The Next Chapter in T-Cell Cancer Immunotherapy. *Biologics* **2021**, *15*, 95. https://doi.org/10.2147/BTT.S291768.

(3)   Belmontes, B.; Sawant, D. V.; Zhong, W.; Tan, H.; Kaul, A.; Aeffner, F.; O'Brien, S. A.; Chun, M.; Noubade, R.; Eng, J.; et al. Immunotherapy Combinations Overcome Resistance to Bispecific T Cell Engager Treatment in T Cell–Cold Solid Tumors. *Sci. Transl. Med.* **2021**, *13* (608), 1524. https://doi.org/10.1126/SCITRANSLMED.ABD1524/SUPPL_FILE/SCITRANSLMED.ABD1524_DATA_FILE_S1.ZIP.

(4)   Zhou, S.; Liu, M.; Ren, F.; Meng, X.; Yu, J. The Landscape of Bispecific T Cell Engager in Cancer Treatment. *Biomark. Res. 2021 91* **2021**, *9* (1), 1–23. https://doi.org/10.1186/S40364-021-00294-9.

(5)   Chen, Y.; Xu, Y. Pharmacokinetics of Bispecific Antibody. *Current Pharmacology Reports*. Springer International Publishing June 1, 2017, pp 126–137. https://doi.org/10.1007/s40495-017-0090-5.

(6)   Chen, Q.; Wang, C.; Chen, G.; Hu, Q.; Gu, Z. Delivery Strategies for Immune Checkpoint Blockade. *Adv. Healthc. Mater.* **2018**, *7* (20), 1800424. https://doi.org/10.1002/ADHM.201800424.

(7)   Dougan, M.; Dougan, S. K. Targeting Immunotherapy to the Tumor Microenvironment. *J. Cell. Biochem.* **2017**, *118* (10), 3049–3054. https://doi.org/10.1002/JCB.26005.

(8)   Esfahani, K.; Roudaia, L.; Buhlaiga, N.; Del Rincon, S. V.; Papneja, N.; Miller, W. H. A Review of Cancer Immunotherapy: From the Past, to the Present, to the Future. *Curr. Oncol.* **2020**, *27* (Suppl 2), S87. https://doi.org/10.3747/CO.27.5223.

(9)   Maia, M. C.; Hansen, A. R. A Comprehensive Review of Immunotherapies in Prostate Cancer. *Crit. Rev. Oncol. Hematol.* **2017**, *113*, 292–303. https://doi.org/10.1016/J.CRITREVONC.2017.02.026.

(10)   Jhunjhunwala, S.; Hammer, C.; Delamarre, L. Antigen Presentation in Cancer: Insights into Tumour Immunogenicity and Immune Evasion. *Nat. Rev. Cancer 2021 215* **2021**, *21* (5), 298–312. https://doi.org/10.1038/s41568-021-00339-z.

(11)   Galluzzi, L.; Vacchelli, E.; Bravo-San Pedro, J. M.; Buqué, A.; Senovilla, L.; Baracco, E. E.; Bloy, N.; Castoldi, F.; Abastado, J. P.; Agostinis, P.; et al. Classification of

Current Anticancer Immunotherapies. *Oncotarget* **2014**, *5* (24), 12472. https://doi.org/10.18632/ONCOTARGET.2998.

(12)   Slaney, C. Y.; Wang, P.; Darcy, P. K.; Kershaw, M. H. CARs versus BiTEs: A Comparison between T Cell–Redirection Strategies for Cancer Treatment. *Cancer Discovery*. American Association for Cancer Research Inc. August 1, 2018, pp 924–934. https://doi.org/10.1158/2159-8290.CD-18-0297.

(13)   Deng, Z.; Wu, Y.; Ma, W.; Zhang, S.; Zhang, Y. Q. Adoptive T-Cell Therapy of Prostate Cancer Targeting the Cancer Stem Cell Antigen EpCAM. *BMC Immunol.* **2015**, *16* (1), 1. https://doi.org/10.1186/s12865-014-0064-x.

(14)   Goebeler, M. E.; Bargou, R. C. T Cell-Engaging Therapies — BiTEs and Beyond. *Nat. Rev. Clin. Oncol.* **2020**, *17* (7), 418–434. https://doi.org/10.1038/s41571-020-0347-5.

(15)   Vafa, O.; Trinklein, N. D. Perspective: Designing T-Cell Engagers With Better Therapeutic Windows. *Front. Oncol.* **2020**, *10*, 446. https://doi.org/10.3389/fonc.2020.00446.

(16)   Friedrich, M.; Raum, T.; Lutterbuese, R.; Voelkel, M.; Deegen, P.; Rau, D.; Kischel, R.; Hoffmann, P.; Brandl, C.; Schuhmacher, J.; et al. Regression of Human Prostate Cancer Xenografts in Mice by AMG 212/BAY2010112, a Novel PSMA/CD3-Bispecific BiTE Antibody Cross-Reactive with Non-Human Primate Antigens. *Mol. Cancer Ther.* **2012**, *11* (12), 2664–2673. https://doi.org/10.1158/1535-7163.MCT-12-0042.

(17)   Deegen, P.; Thomas, O.; Nolan-Stevaux, O.; Li, S.; Wahl, J.; Bogner, P.; Aeffner, F.; Friedrich, M.; Liao, M. Z.; Matthes, K.; et al. The PSMA-Targeting Half-Life Extended BiTE Therapy AMG 160 Has Potent Antitumor Activity in Preclinical Models of Metastatic Castration-Resistant Prostate Cancer. *Clin. Cancer Res.* **2021**, *27* (10), 2928–2937. https://doi.org/10.1158/1078-0432.CCR-20-3725/78963/AM/THE-PSMA-TARGETING-HALF-LIFE-EXTENDED-BITER.

(18)   Rosenthal, M.; Balana, C.; Linde, M. E. Van; Sayehli, C.; Fiedler, W. M.; Wermke, M.; Massard, C.; Ang, A.; Kast, J.; Stienen, S.; et al. Novel Anti-EGFRvIII Bispecific T Cell Engager (BiTE) Antibody Construct in Glioblastoma (GBM): Trial in Progress of AMG 596 in Patients with Recurrent or Newly Diagnosed Disease. *https://doi.org/10.1200/JCO.2019.37.15_suppl.TPS2071* **2019**, *37* (15_suppl), TPS2071–TPS2071. https://doi.org/10.1200/JCO.2019.37.15_SUPPL.TPS2071.

(19)   Giffin, M. J.; Cooke, K.; Lobenhofer, E. K.; Estrada, J.; Zhan, J.; Deegen, P.; Thomas, M.; Murawsky, C. M.; Werner, J.; Liu, S.; et al. AMG 757, a Half-Life Extended, DLL3-Targeted Bispecific T-Cell Engager, Shows High Potency and Sensitivity in Preclinical Models of Small-Cell Lung Cancer. *Clin. Cancer Res.* **2021**, *27* (5), 1526–

1537. https://doi.org/10.1158/1078-0432.CCR-20-2845/78594/AM/AMG-757-A-HALF-LIFE-EXTENDED-DLL3-TARGETED.

(20) Chao, J.; Buxó, E.; Cervantes, A.; Dayyani, F.; Lima, C. M. S. P. R.; Greil, R.; Laarhoven, H. W. M. Van; Lorenzen, S.; Heinemann, V.; Kischel, R.; et al. Trial in Progress: A Phase I Study of AMG 199, a Half-Life Extended Bispecific T-Cell Engager (HLE BiTE) Immune Therapy, Targeting MUC17 in Patients with Gastric and Gastroesophageal Junction (G/GEJ) Cancer. *https://doi.org/10.1200/JCO.2020.38.15_suppl.TPS4649* **2020**, *38* (15_suppl), TPS4649–TPS4649. https://doi.org/10.1200/JCO.2020.38.15_SUPPL.TPS4649.

(21) Topp, M. S.; Gökbuget, N.; Zugmaier, G.; Klappers, P.; Stelljes, M.; Neumann, S.; Viardot, A.; Marks, R.; Diedrich, H.; Faul, C.; et al. Phase II Trial of the Anti-CD19 Bispecific T Cell-Engager Blinatumomab Shows Hematologic and Molecular Remissions in Patients With Relapsed or Refractory B-Precursor Acute Lymphoblastic Leukemia. *J Clin Oncol* **2014**, *32*, 4134–4140. https://doi.org/10.1200/JCO.2014.56.3247.

(22) Topp, M. S.; Gökbuget, N.; Stein, A. S.; Zugmaier, G.; O'Brien, S.; Bargou, R. C.; Dombret, H.; Fielding, A. K.; Heffner, L.; Larson, R. A.; et al. Safety and Activity of Blinatumomab for Adult Patients with Relapsed or Refractory B-Precursor Acute Lymphoblastic Leukaemia: A Multicentre, Single-Arm, Phase 2 Study. *Lancet Oncol.* **2015**, *16* (1), 57–66. https://doi.org/10.1016/S1470-2045(14)71170-2.

(23) Von Stackelberg, A.; Locatelli, F.; Zugmaier, G.; Handgretinger, R.; Trippett, T. M.; Rizzari, C.; Bader, P.; O'brien, M. M.; Brethon, B.; Bhojwani, D.; et al. Phase I/Phase II Study of Blinatumomab in Pediatric Patients with Relapsed/Refractory Acute Lymphoblastic Leukemia. *J. Clin. Oncol.* **2016**, *34* (36), 4381–4389. https://doi.org/10.1200/JCO.2016.67.3301.

(24) Baeuerle, P. A.; Reinhardt, C. Bispecific T-Cell Engaging Antibodies for Cancer Therapy. *Cancer Research*. American Association for Cancer Research June 15, 2009, pp 4941–4944. https://doi.org/10.1158/0008-5472.CAN-09-0547.

(25) Suryadevara, C. M.; Gedeon, P. C.; Sanchez-Perez, L.; Verla, T.; Alvarez-Breckenridge, C.; Choi, B. D.; Fecci, P. E.; Sampson, J. H. Are BiTEs the "Missing Link" in Cancer Therapy? *OncoImmunology*. Taylor and Francis Inc. January 1, 2015. https://doi.org/10.1080/2162402X.2015.1008339.

(26) Klinger, M.; Brandl, C.; Zugmaier, G.; Hijazi, Y.; Bargou, R. C.; Topp, M. S.; Gökbuget, N.; Neumann, S.; Goebeler, M.; Viardot, A.; et al. Immunopharmacologic Response of Patients with B-Lineage Acute Lymphoblastic Leukemia to Continuous Infusion of T Cell–Engaging CD19/CD3-Bispecific BiTE Antibody Blinatumomab. *Blood* **2012**, *119* (26), 6226–6233. https://doi.org/10.1182/BLOOD-2012-01-400515.

(27) Arvedson, T.; Bailis, J. M.; Britten, C. D.; Klinger, M.; Nagorsen, D.; Coxon, A.; Egen, J. G.; Martin, F. Targeting Solid Tumors with Bispecific T Cell Engager Immune Therapy. **2022**. https://doi.org/10.1146/annurev-cancerbio-070620.

(28) Kebenko, M.; Goebeler, M. E.; Wolf, M.; Hasenburg, A.; Seggewiss-Bernhardt, R.; Ritter, B.; Rautenberg, B.; Atanackovic, D.; Kratzer, A.; Rottman, J. B.; et al. A Multicenter Phase 1 Study of Solitomab (MT110, AMG 110), a Bispecific EpCAM/CD3 T-Cell Engager (BiTE®) Antibody Construct, in Patients with Refractory Solid Tumors. *Oncoimmunology* **2018**, *7* (8). https://doi.org/10.1080/2162402X.2018.1450710/SUPPL_FILE/KONI_A_1450710_SM6136.DOCX.

(29) Tran, B.; Horvath, L.; Rettig, M.; Fizazi, K.; Lolkema, M. P.; Dorff, T. B.; Greil, R.; Machiels, J.-P. H.; Autio, K. A.; Rottey, S.; et al. Phase I Study of AMG 160, a Half-Life Extended Bispecific T-Cell Engager (HLE BiTE Immune Therapy) Targeting Prostate-Specific Membrane Antigen, in Patients with Metastatic Castration-Resistant Prostate Cancer (MCRPC). *https://doi.org/10.1200/JCO.2020.38.15_suppl.TPS5590* **2020**, *38* (15_suppl), TPS5590–TPS5590. https://doi.org/10.1200/JCO.2020.38.15_SUPPL.TPS5590.

(30) Yuan, H.; Jiang, W.; Von Roemeling, C. A.; Qie, Y.; Liu, X.; Chen, Y.; Wang, Y.; Wharen, R. E.; Yun, K.; Bu, G.; et al. Multivalent Bi-Specific Nanobioconjugate Engager for Targeted Cancer Immunotherapy. *Nat. Nanotechnol.* **2017**, *12* (8), 763–769. https://doi.org/10.1038/nnano.2017.69.

(31) Scott, E. M.; Jacobus, E. J.; Lyons, B.; Frost, S.; Freedman, J. D.; Dyer, A.; Khalique, H.; Taverner, W. K.; Carr, A.; Champion, B. R.; et al. Bi- And Tri-Valent T Cell Engagers Deplete Tumour-Associated Macrophages in Cancer Patient Samples. *J. Immunother. Cancer* **2019**, *7* (1), 1–18. https://doi.org/10.1186/S40425-019-0807-6/FIGURES/7.

(32) Alhallak, K.; O'Neal, J.; Sun, J.; Muz, B.; King, J.; Kohnen, D.; Achilefu, S.; Vij, R.; DiPersio, J.; Azab, K. Nanoparticle Multi-Specific T Cell Engagers for the Treatment of Multiple Myeloma. *Clin. Lymphoma Myeloma Leuk.* **2019**, *19* (10), e156. https://doi.org/10.1016/J.CLML.2019.09.260.

(33) Slaga, D.; Ellerman, D.; Lombana, T. N.; Vij, R.; Li, J.; Hristopoulos, M.; Clark, R.; Johnston, J.; Shelton, A.; Mai, E.; et al. Avidity-Based Binding to HER2 Results in Selective Killing of HER2-Overexpressing Cells by Anti-HER2/CD3. *Sci. Transl. Med.* **2018**, *10* (463). https://doi.org/10.1126/scitranslmed.aat5775.

(34) Hong, S.; Leroueil, P. R.; Majoros, I. J.; Orr, B. G.; Baker, J. R.; Banaszak Holl, M. M. The Binding Avidity of a Nanoparticle-Based Multivalent Targeted Drug Delivery Platform. *Chem. Biol.* **2007**, *14* (1), 107–115. https://doi.org/10.1016/j.chembiol.2006.11.015.

(35) Schütz, C.; Varela, J. C.; Perica, K.; Haupt, C.; Oelke, M.; Schneck, J. P. Antigen-Specific T Cell Redirectors: A Nanoparticle Based Approach for Redirecting T Cells. *Oncotarget* **2016**, *7* (42), 68503. https://doi.org/10.18632/ONCOTARGET.11785.

(36) Panchal, A.; Seto, P.; Wall, R.; Hillier, B. J.; Zhu, Y.; Krakow, J.; Datt, A.; Pongo, E.; Bagheri, A.; Chen, T. H. T.; et al. COBRA[TM]: A Highly Potent Conditionally Active T Cell Engager Engineered for the Treatment of Solid Tumors. *MAbs* **2020**, *12* (1). https://doi.org/10.1080/19420862.2020.1792130/SUPPL_FILE/KMAB_A_1792130_SM4073.ZIP.

(37) Choi, B. D.; Yu, X.; Castano, A. P.; Bouffard, A. A.; Schmidts, A.; Larson, R. C.; Bailey, S. R.; Boroughs, A. C.; Frigault, M. J.; Leick, M. B.; et al. CAR-T Cells Secreting BiTEs Circumvent Antigen Escape without Detectable Toxicity. *Nat. Biotechnol. 2019 379* **2019**, *37* (9), 1049–1058. https://doi.org/10.1038/s41587-019-0192-1.

(38) Scott, E. M.; Duffy, M. R.; Freedman, J. D.; Fisher, K. D.; Seymour, L. W.; Scott, E. M.; Duffy, M. R.; Freedman, J. D.; Fisher, K. D.; Seymour, L. W. Solid Tumor Immunotherapy with T Cell Engager-Armed Oncolytic Viruses. *Macromol. Biosci.* **2018**, *18* (1), 1700187. https://doi.org/10.1002/MABI.201700187.

(39) Barlabé, P.; Sostoa, J. de; Fajardo, C. A.; Alemany, R.; Moreno, R. Enhanced Antitumor Efficacy of an Oncolytic Adenovirus Armed with an EGFR-Targeted BiTE Using Menstrual Blood-Derived Mesenchymal Stem Cells as Carriers. *Cancer Gene Ther. 2019 275* **2019**, *27* (5), 383–388. https://doi.org/10.1038/s41417-019-0110-1.

(40) Fierle, J. K.; Brioschi, M.; de Tiani, M.; Wetterwald, L.; Atsaves, V.; Abram-Saliba, J.; Petrova, T. V.; Coukos, G.; Dunn, S. M. Soluble Trivalent Engagers Redirect Cytolytic T Cell Activity toward Tumor Endothelial Marker 1. *Cell Reports Med.* **2021**, *2* (8), 100362. https://doi.org/10.1016/J.XCRM.2021.100362.

(41) Cheng, P.; Chen, X.; Dalton, R.; Calescibetta, A.; So, T.; Gilvary, D.; Ward, G.; Smith, V.; Eckard, S.; Fox, J. A.; et al. Immunodepletion of MDSC by AMV564, a Novel Bivalent, Bispecific CD33/CD3 T Cell Engager, Ex Vivo in MDS and Melanoma. *Mol. Ther.* **2022**, *30* (6), 2315–2326. https://doi.org/10.1016/J.YMTHE.2022.02.005.

(42) Alhallak, K.; Sun, J.; Wasden, K.; Guenthner, N.; O'Neal, J.; Muz, B.; King, J.; Kohnen, D.; Vij, R.; Achilefu, S.; et al. Nanoparticle T-Cell Engagers as a Modular Platform for Cancer Immunotherapy. *Leuk. 2021 358* **2021**, *35* (8), 2346–2357. https://doi.org/10.1038/s41375-021-01127-2.

(43) Guimarães, D.; Cavaco-Paulo, A.; Nogueira, E. Design of Liposomes as Drug Delivery System for Therapeutic Applications. *Int. J. Pharm.* **2021**, *601*, 120571. https://doi.org/10.1016/J.IJPHARM.2021.120571.

(44) Fransen, M. F.; Van Der Sluis, T. C.; Ossendorp, F.; Arens, R.; Melief, C. J. M. Controlled Local Delivery of CTLA-4 Blocking Antibody Induces CD8 + T-Cell-Dependent Tumor Eradication and Decreases Risk of Toxic Side Effects. *Clin. Cancer Res.* **2013**, *19* (19), 5381–5389. https://doi.org/10.1158/1078-0432.CCR-12-0781/286121/AM/CONTROLLED-LOCAL-DELIVERY-OF-CTLA-4-BLOCKING.

(45) Li, Y.; Fang, M.; Zhang, J.; Wang, J.; Song, Y.; Shi, J.; Li, W.; Wu, G.; Ren, J.; Wang, Z.; et al. Hydrogel Dual Delivered Celecoxib and Anti-PD-1 Synergistically Improve Antitumor Immunity. *Oncoimmunology* **2016**, *5* (2). https://doi.org/10.1080/2162402X.2015.1074374/SUPPL_FILE/KONI_A_1074374_SM2321.ZIP.

(46) Fransen, M. F.; Sluijter, M.; Morreau, H.; Arens, R.; Melief, C. J. M. Local Activation of CD8 T Cells and Systemic Tumor Eradication without Toxicity via Slow Release and Local Delivery of Agonistic CD40 Antibody. *Clin. Cancer Res.* **2011**, *17* (8), 2270–2280. https://doi.org/10.1158/1078-0432.CCR-10-2888/84115/AM/LOCAL-REPROGRAMMING-OF-CD8-T-CELLS-AND-SYSTEMIC.

(47) Ma, H.; He, C.; Chen Ma, X. H.; He, C.; Chen, X.; Ma, H. Injectable Hydrogels as Local Depots at Tumor Sites for Antitumor Immunotherapy and Immune-Based Combination Therapy. *Macromol. Biosci.* **2021**, *21* (6), 2100039. https://doi.org/10.1002/MABI.202100039.

(48) Momin, N.; Palmeri, J. R.; Lutz, E. A.; Jailkhani, N.; Mak, H.; Tabet, A.; Chinn, M. M.; Kang, B. H.; Spanoudaki, V.; Hynes, R. O.; et al. Maximizing Response to Intratumoral Immunotherapy in Mice by Tuning Local Retention. *Nat. Commun. 2022 131* **2022**, *13* (1), 1–13. https://doi.org/10.1038/s41467-021-27390-6.

(49) Wu, L.; Seung, E.; Xu, L.; Rao, E.; Lord, D. M.; Wei, R. R.; Cortez-Retamozo, V.; Ospina, B.; Posternak, V.; Ulinski, G.; et al. Trispecific Antibodies Enhance the Therapeutic Efficacy of Tumor-Directed T Cells through T Cell Receptor Co-Stimulation. *Nat. Cancer 2019 11* **2019**, *1* (1), 86–98. https://doi.org/10.1038/s43018-019-0004-z.

(50) Zekri, L.; Vogt, F.; Osburg, L.; Müller, S.; Kauer, J.; Manz, T.; Pflügler, M.; Maurer, A.; Heitmann, J. S.; Hagelstein, I.; et al. An IgG-Based Bispecific Antibody for Improved Dual Targeting in PSMA-Positive Cancer. *EMBO Mol. Med.* **2021**, *13* (2), e11902. https://doi.org/10.15252/EMMM.201911902.

(51) Veronese, F. M.; Mero, A. The Impact of PEGylation on Biological Therapies. *BioDrugs* **2008**, *22* (5), 315–329. https://doi.org/10.2165/00063030-200822050-00004/FIGURES/7.

(52) Gupta, V.; Bhavanasi, S.; Quadir, M.; Singh, K.; Ghosh, G.; Vasamreddy, K.; Ghosh, A.; Siahaan, T. J.; Banerjee, S.; Banerjee, S. K. Protein PEGylation for Cancer

Therapy: Bench to Bedside. *J. Cell Commun. Signal.* **2019**, *13* (3), 319. https://doi.org/10.1007/S12079-018-0492-0.

(53)   Wang, Y.; Cooke, M. J.; Lapitsky, Y.; Wylie, R. G.; Sachewsky, N.; Corbett, D.; Morshead, C. M.; Shoichet, M. S. Transport of Epidermal Growth Factor in the Stroke-Injured Brain. *J. Control. Release* **2011**, *149* (3), 225–235. https://doi.org/10.1016/J.JCONREL.2010.10.022.

(54)   Shoaib, M. M.; Huynh, V.; Shad, Y.; Ahmed, R.; Jesmer, A. H.; Melacini, G.; Wylie, R. G. Controlled Degradation of Low-Fouling Poly(Oligo(Ethylene Glycol)Methyl Ether Methacrylate) Hydrogels †. **2019**. https://doi.org/10.1039/c9ra03441b.

(55)   Aina, O. H.; Sroka, T. C.; Chen, M. L.; Lam, K. S. Therapeutic Cancer Targeting Peptides. *Pept. Sci.* **2002**, *66* (3), 184–199. https://doi.org/10.1002/BIP.10257.

(56)   Wang, S. H.; Yu, J. Structure-Based Design for Binding Peptides in Anti-Cancer Therapy. *Biomaterials* **2018**, *156*, 1–15. https://doi.org/10.1016/J.BIOMATERIALS.2017.11.024.

(57)   Gourni, E.; Henriksen, G.; Gamez, P.; Caballero, A. B. Metal-Based PSMA Radioligands. *Mol. 2017, Vol. 22, Page 523* **2017**, *22* (4), 523. https://doi.org/10.3390/MOLECULES22040523.

(58)   Aina, O. H.; Liu, R.; Sutcliffe, J. L.; Marik, J.; Pan, C. X.; Lam, K. S. From Combinatorial Chemistry to Cancer-Targeting Peptides. *Mol. Pharm.* **2007**, *4* (5), 631–651. https://doi.org/10.1021/MP700073Y/ASSET/IMAGES/LARGE/MP-2007-00073Y_0010.JPEG.

(59)   Liu, R.; Li, X.; Xiao, W.; Lam, K. S. Tumor-Targeting Peptides from Combinatorial Libraries. *Adv. Drug Deliv. Rev.* **2017**, *110–111*, 13–37. https://doi.org/10.1016/J.ADDR.2016.05.009.

(60)   Kwon, Y. Do; Chung, H. J.; Lee, S. J.; Lee, S. H.; Jeong, B. H.; Kim, H. K. Synthesis of Novel Multivalent Fluorescent Inhibitors with High Affinity to Prostate Cancer and Their Biological Evaluation. *Bioorg. Med. Chem. Lett.* **2018**, *28* (4), 572–576. https://doi.org/10.1016/J.BMCL.2018.01.047.

(61)   Saniee, F.; Shabani Ravari, N.; Goodarzi, N.; Amini, M.; Atyabi, F.; Saeedian Moghadam, E.; Dinarvand, R. Glutamate-Urea-Based PSMA-Targeted PLGA Nanoparticles for Prostate Cancer Delivery of Docetaxel. *Pharm. Dev. Technol.* **2021**, *26* (4), 381–389. https://doi.org/10.1080/10837450.2021.1875238.

(62)   Huang, B.; Otis, J.; Joice, M.; Kotlyar, A.; Thomas, T. P. PSMA-Targeted Stably Linked "Dendrimer-Glutamate Urea-Methotrexate" as a Prostate Cancer Therapeutic. **2014**. https://doi.org/10.1021/bm401777w.

(63) Kozikowski, A.; Conti, P.; Jh, Z. Design of Remarkably Simple, Yet Potent Urea-Based Inhibitors of Glutamate Carboxypeptidase II (NAALADase) Procognitive Efficacy of NAAG Acting at MGluR3 View Project 5-HT2C-Agonists View Project. *Artic. J. Med. Chem.* **2001**. https://doi.org/10.1021/jm000406m.

(64) Oberg, H. H.; Kellner, C.; Gonnermann, D.; Peipp, M.; Peters, C.; Sebens, S.; Kabelitz, D.; Wesch, D. Γδ T Cell Activation by Bispecific Antibodies. *Cell. Immunol.* **2015**, *296* (1), 41–49. https://doi.org/10.1016/J.CELLIMM.2015.04.009.

(65) Runcie, K.; Budman, D. R.; John, V.; Seetharamu, N. Bi-Specific and Tri-Specific Antibodies- the next Big Thing in Solid Tumor Therapeutics. *Mol. Med.* **2018**, *24* (1), 1–15. https://doi.org/10.1186/S10020-018-0051-4/TABLES/5.

(66) Fu, M.; He, Q.; Guo, Z.; Zhou, X.; Li, H.; Zhao, L.; Tang, H.; Zhou, X.; Zhu, H.; Shen, G.; et al. Therapeutic Bispecific T-Cell Engager Antibody Targeting the Transferrin Receptor. *Front. Immunol.* **2019**, *10* (JUN), 1396. https://doi.org/10.3389/fimmu.2019.01396.

(67) Chapman, A. P. PEGylated Antibodies and Antibody Fragments for Improved Therapy: A Review. *Adv. Drug Deliv. Rev.* **2002**, *54* (4), 531–545. https://doi.org/10.1016/S0169-409X(02)00026-1.

(68) Ton, N. C.; Parker, G. J. M.; Jackson, A.; Mullamitha, S.; Buonaccorsi, G. A.; Roberts, C.; Watson, Y.; Davies, K.; Cheung, S.; Hope, L.; et al. Phase I Evaluation of CDP791, a PEGylated Di-Fab' Conjugate That Binds Vascular Endothelial Growth Factor Receptor 2. *Clin. Cancer Res.* **2007**, *13* (23), 7113–7118. https://doi.org/10.1158/1078-0432.CCR-07-1550.

(69) Tsourlakis, M. C.; Klein, F.; Kluth, M.; Quaas, A.; Graefen, M.; Haese, A.; Simon, R.; Sauter, G.; Schlomm, T.; Minner, S. PSMA Expression Is Highly Homogenous in Primary Prostate Cancer. *Appl. Immunohistochem. Mol. Morphol.* **2015**, *23* (6), 449–455. https://doi.org/10.1097/PAI.0000000000000110.

(70) Xu, B.; Zhou, F.; Yan, M. M.; Cai, D. S.; Guo, W. B.; Yang, Y. Q.; Jia, X. H.; Zhang, W. X.; Li, T.; Ma, T.; et al. PSMA-Oriented Target Delivery of Novel Anticancer Prodrugs: Design, Synthesis, and Biological Evaluations of Oligopeptide-Camptothecin Conjugates. *Int. J. Mol. Sci. 2018, Vol. 19, Page 3251* **2018**, *19* (10), 3251. https://doi.org/10.3390/IJMS19103251.

(71) Kubetzko, S.; Sarkar, C. A.; Pï, A. Protein PEGylation Decreases Observed Target Association Rates via a Dual Blocking Mechanism □ S. **2005**. https://doi.org/10.1124/mol.105.014910.

(72) Chen, B. M.; Al-Aghbar, M. A.; Lee, C. H.; Chang, T. C.; Su, Y. C.; Li, Y. C.; Chang, S. E.; Chen, C. C.; Chung, T. H.; Liao, Y. C.; et al. The Affinity of Elongated Membrane-

Tethered Ligands Determines Potency of T Cell Receptor Triggering. *Front. Immunol.* **2017**, *8* (JUL), 793. https://doi.org/10.3389/FIMMU.2017.00793/BIBTEX.

(73) Hexham, J. M.; Dudas, D.; Hugo, R.; Thompson, J.; King, V.; Dowling, C.; Neville, D. M.; Digan, M. E.; Lake, P. Influence of Relative Binding Affinity on Efficacy in a Panel of Anti-CD3 ScFv Immunotoxins. *Mol. Immunol.* **2001**, *38* (5), 397–408. https://doi.org/10.1016/S0161-5890(01)00070-0.

(74) Verwilghen, J.; Baroja, M. L.; Van Vaeck, F.; Van Damme, J.; Ceuppens, J. L. Differences in the Stimulating Capacity of Immobilized Anti-CD3 Monoclonal Antibodies: Variable Dependence on Interleukin-1 as a Helper Signal for T-Cell Activation. *Immunology* **1991**, *72*, 269–276.

(75) Jesmer, A. H.; Huynh, V.; Marple, A. S. T.; Ding, X.; Moran-Mirabal, J. M.; Wylie, R. G. Graft-Then-Shrink: Simultaneous Generation of Antifouling Polymeric Interfaces and Localized Surface Plasmon Resonance Biosensors. *ACS Appl. Mater. Interfaces* **2021**, *13* (44), 52362–52373. https://doi.org/10.1021/acsami.1c14930.

(76) Bluemel, C.; Hausmann, S.; Fluhr, P.; Sriskandarajah, M.; Stallcup, W. B.; Baeuerle, P. A.; Kufer, P. Epitope Distance to the Target Cell Membrane and Antigen Size Determine the Potency of T Cell-Mediated Lysis by BiTE Antibodies Specific for a Large Melanoma Surface Antigen. *Cancer Immunol. Immunother.* **2010**, *59* (8), 1197–1209. https://doi.org/10.1007/S00262-010-0844-Y/FIGURES/6.

(77) Shaw, A. S.; Dustin, M. L. Making the T Cell Receptor Go the Distance: Review A Topological View of T Cell Activation. *Immunity* **1997**, *6*, 361–369.

(78) Klein, J. S.; Gnanapragasam, P. N. P.; Galimidi, R. P.; Foglesong, C. P.; West, A. P.; Bjorkman, P. J. Examination of the Contributions of Size and Avidity to the Neutralization Mechanisms of the Anti-HIV Antibodies B12 and 4E10. *Proc. Natl. Acad. Sci. U. S. A.* **2009**, *106* (18), 7385–7390. https://doi.org/10.1073/PNAS.0811427106/SUPPL_FILE/0811427106SI.PDF.

(79) Yamada, S.; Sanada, Y.; Tamura, A.; Yui, N.; Sakurai, K. Chain Architecture and Flexibility of α-Cyclodextrin/PEG Polyrotaxanes in Dilute Solutions. *Polym. J.* **2015**, *47*, 464–467. https://doi.org/10.1038/pj.2015.18.

(80) Miller, B. R.; Demarest, S. J.; Lugovskoy, A.; Huang, F.; Wu, X.; Snyder, W. B.; Croner, L. J.; Wang, N.; Amatucci, A.; Michaelson, J. S.; et al. Stability Engineering of ScFvs for the Development of Bispecific and Multivalent Antibodies. *Protein Eng. Des. Sel.* **2010**, *23* (7), 549–557. https://doi.org/10.1093/PROTEIN/GZQ028.

(81) Wang, Q.; Chen, Y.; Park, J.; Liu, X.; Hu, Y.; Wang, T.; McFarland, K.; Betenbaugh, M. J. Design and Production of Bispecific Antibodies. *Antibodies* **2019**, *8* (3), 43.

https://doi.org/10.3390/ANTIB8030043.

(82) Baalmann, M.; aura Neises, L.; ebastian Bitsch, S.; Schneider, H.; Deweid, L.; Werther, P.; Ilkenhans, N.; Wolfring, M.; ichael Ziegler, M. J.; onas Wilhelm, J.; et al. A Bioorthogonal Click Chemistry Toolbox for Targeted Synthesis of Branched and Well-Defined Protein–Protein Conjugates. *Angew. Chemie* **2020**, *132* (31), 12985–12993. https://doi.org/10.1002/ANGE.201915079.

(83) Tapan K. Bera; Jaye Viner; Elisabeth Brinkmann; Ira Pastan. Pharmacokinetics and Antitumor Activity of a Bivalent Disulfide-Stabilized Fv Immunotoxin with Improved Antigen Binding to ErbB2 | Cancer Research | American Association for Cancer Research. *Cancer Res.* **1999**, *59* (16), 4018–4022.

(84) Vernimmen, D.; Gueders, M.; Pisvin, S.; Delvenne, P.; Winkler, R. Different Mechanisms Are Implicated in ERBB2 Gene Overexpression in Breast and in Other Cancers. *Br. J. Cancer 2003 895* **2003**, *89* (5), 899–906. https://doi.org/10.1038/sj.bjc.6601200.

(85) Chelobanov, B.; Poletaeva, J.; Epanchintseva, A.; Tupitsyna, A.; Pyshnaya, I.; Ryabchikova, E. Ultrastructural Features of Gold Nanoparticles Interaction with HepG2 and HEK293 Cells in Monolayer and Spheroids. *Nanomater. 2020, Vol. 10, Page 2040* **2020**, *10* (10), 2040. https://doi.org/10.3390/NANO10102040.

(86) Liu, C. C.; Schultz, P. G. Adding New Chemistries to the Genetic Code. *http://dx.doi.org/10.1146/annurev.biochem.052308.105824* **2010**, *79*, 413–444. https://doi.org/10.1146/ANNUREV.BIOCHEM.052308.105824.

(87) Schumacher, D.; Hackenberger, C. P. R.; Leonhardt, H.; Helma, J. Current Status: Site-Specific Antibody Drug Conjugates. *J. Clin. Immunol.* **2016**, *36* (1), 100–107. https://doi.org/10.1007/S10875-016-0265-6/FIGURES/2.

(88) Axup, J. Y.; Bajjuri, K. M.; Ritland, M.; Hutchins, B. M.; Kim, C. H.; Kazane, S. A.; Halder, R.; Forsyth, J. S.; Santidrian, A. F.; Stafin, K.; et al. Synthesis of Site-Specific Antibody-Drug Conjugates Using Unnatural Amino Acids. *Proc. Natl. Acad. Sci. U. S. A.* **2012**, *109* (40), 16101–16106. https://doi.org/10.1073/PNAS.1211023109/SUPPL_FILE/PNAS.201211023SI.PDF.

(89) Ramakrishnan, B.; Qasba, P. K. Structure-Based Design of B1,4-Galactosyltransferase I (B4Gal-T1) with Equally Efficient N-Acetylgalactosaminyltransferase Activity: POINT MUTATION BROADENS B4Gal-T1 DONOR SPECIFICITY *. *J. Biol. Chem.* **2002**, *277* (23), 20833–20839. https://doi.org/10.1074/JBC.M111183200.

(90) Boeggeman, E.; Ramakrishnan, B.; Pasek, M.; Manzoni, M.; Puri, A.; Loomis, K. H.; Waybright, T. J.; Qasba, P. K. Site Specific Conjugation of Fluoroprobes to the

Remodeled Fc N-Glycans of Monoclonal Antibodies Using Mutant Glycosyltransferases: Application for Cell Surface Antigen Detection. https://doi.org/10.1021/bc900103p.

(91)   Smith-Garvin, J. E.; Koretzky, G. A.; Jordan, M. S. T Cell Activation. *Annu. Rev. Immunol.* **2009**, *27*, 591. https://doi.org/10.1146/ANNUREV.IMMUNOL.021908.132706.

(92)   Skokos, D.; Waite, J. C.; Haber, L.; Crawford, A.; Hermann, A.; Ullman, E.; Slim, R.; Godin, S.; Ajithdoss, D.; Ye, X.; et al. A Class of Costimulatory CD28-Bispecific Antibodies That Enhance the Antitumor Activity of CD3-Bispecific Antibodies. *Sci. Transl. Med.* **2020**, *12* (525), 7888. https://doi.org/10.1126/SCITRANSLMED.AAW7888/SUPPL_FILE/AAW7888_SM.PDF.

(93)   Laszlo, G. S.; Gudgeon, C. J.; Harrington, K. H.; Walter, R. B. T-Cell Ligands Modulate the Cytolytic Activity of the CD33/CD3 BiTE Antibody Construct, AMG 330. *Blood Cancer J. 2015 58* **2015**, *5* (8), e340–e340. https://doi.org/10.1038/bcj.2015.68.

(94)   Correnti, C. E.; Laszlo, G. S.; De Van Der Schueren, W. J.; Godwin, C. D.; Ashok Bandaranayake, •; Busch, M. A.; Gudgeon, C. J.; Bates, O. M.; Olson, J. M.; Mehlin, • Christopher; et al. Simultaneous Multiple Interaction T-Cell Engaging (SMITE) Bispecific Antibodies Overcome Bispecific T-Cell Engager (BiTE) Resistance via CD28 Co-Stimulation. *Leukemia* **2018**, *32*, 1239–1243. https://doi.org/10.1038/s41375-018-0014-3.

(95)   Hornig, N.; Reinhardt, K.; Kermer, V.; Kontermann, R. E.; Müller, D. Evaluating Combinations of Costimulatory Antibody-Ligand Fusion Proteins for Targeted Cancer Immunotherapy. *Cancer Immunol. Immunother.* **2013**, *62* (8), 1369–1380. https://doi.org/10.1007/S00262-013-1441-7/FIGURES/5.

(96)   Arndt, C.; Feldmann, A.; Von Bonin, M.; Cartellieri, M.; Ewen, E. M.; Koristka, S.; Michalk, I.; Stamova, S.; Berndt, N.; Gocht, A.; et al. Costimulation Improves the Killing Capability of T Cells Redirected to Tumor Cells Expressing Low Levels of CD33: Description of a Novel Modular Targeting System. *Leuk. 2014 281* **2013**, *28* (1), 59–69. https://doi.org/10.1038/leu.2013.243.

(97)   Zhukovsky, E. A.; Morse, R. J.; Maus, M. V. Bispecific Antibodies and CARs: Generalized Immunotherapeutics Harnessing T Cell Redirection. *Curr. Opin. Immunol.* **2016**, *40*, 24–35. https://doi.org/10.1016/J.COI.2016.02.006.

Appendix
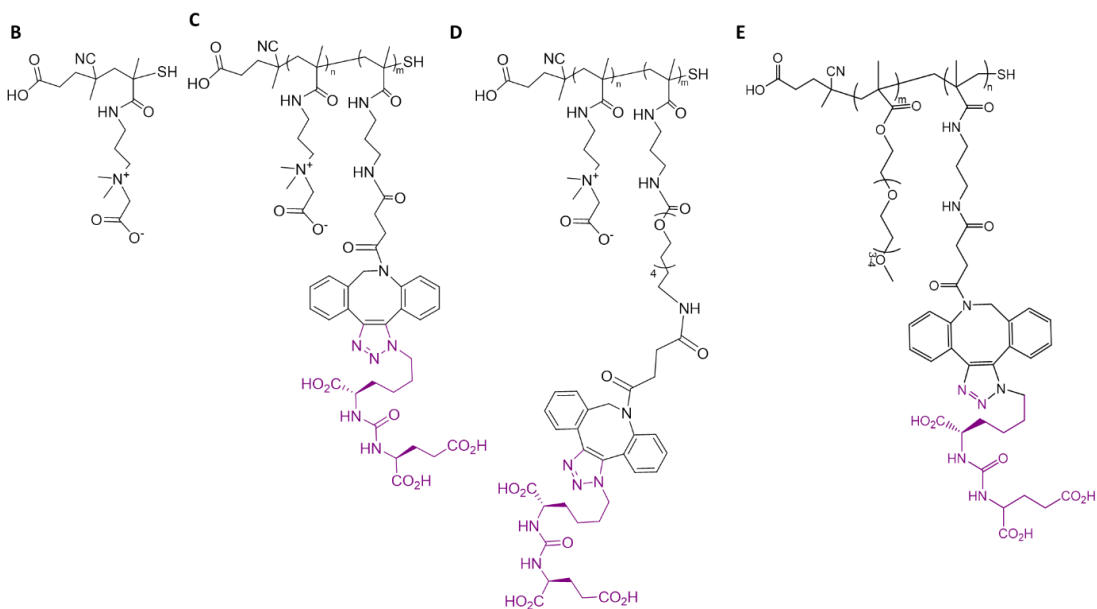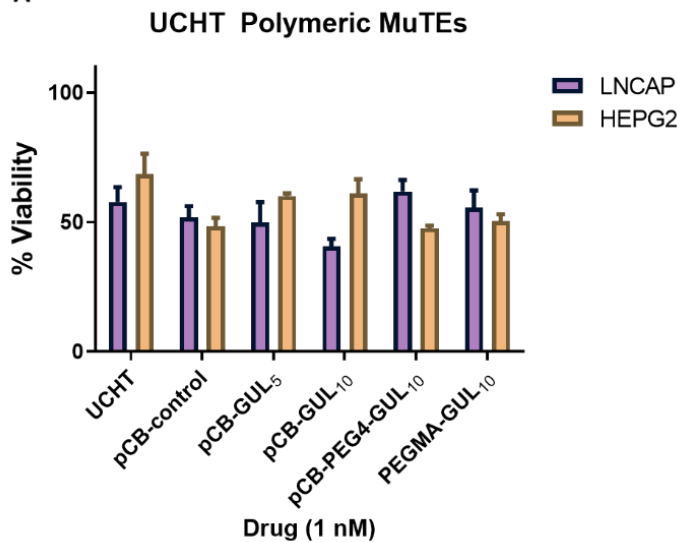
0.1 Figure S1. Polymeric MuTEs do not have targeted cytotoxicity.

Polymer chains with or without PSMA targeting GUL ligands were conjugated to UCHT-1 anti-CD3 antibody (via thiol-maleimide chemistry) to create polymeric MuTEs. A) Polymeric MuTEs do not reduce the toxicity of the anti-CD3 antibody. Cancer cells and T cells incubated at a 5:1 E:T Ratio, with 1 nM drug, n=3 mean ± SD. Polymer structures shown below B) pCB-control (homo-polymer, no targeting ligand), C) pCB-GUL copolymer (5-10 mol% GUL content), D) pCB-PEG4-GUL polymer (10 mol% GUL), E) P(EG)4/5MA-GUL copolymer (10 mol% GUL).
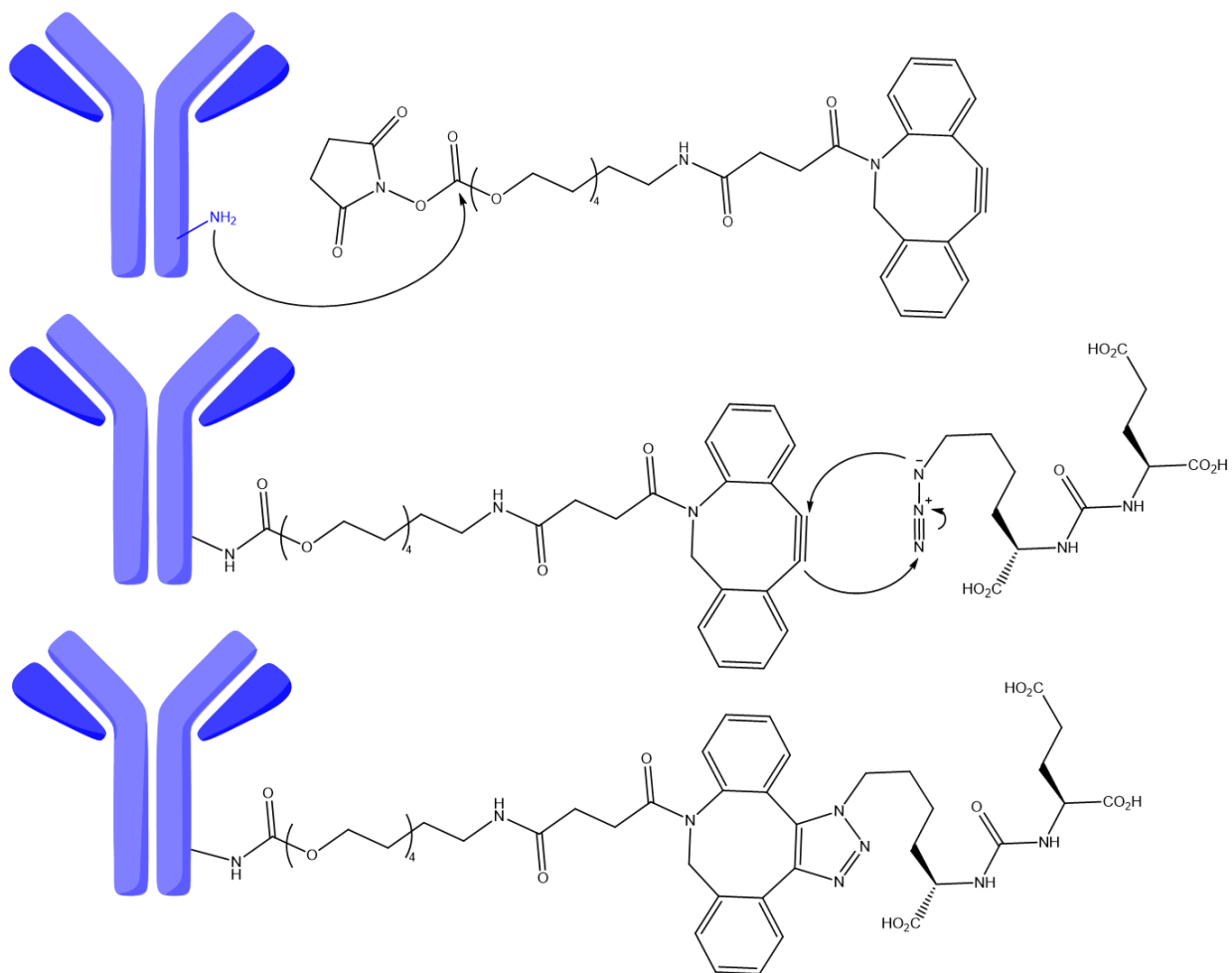
0.2 Figure S2. Two step synthesis of Linker Grafted MuTEs.

1) Addition of short heterobifunctional linkers vis NHS-ester and amines present on the anti-CD3 antibody. 2) Conjugation of cancer targeting peptide (GUL-Az) via SPAAC.

Table S1- Summary of MuTE Binding.

Grafting Density *(# EO-GUL/Ab)	Association	Dissociation	% Viability of LNCaP (PSMA +ve)	% Viability of HEPG2 (PSMA -ve)
0	None	N/A	46	52
1-2	Low	Complete	56	51
~22	High	None	98	95

*In all conditions the non-targeting MuTE showed no association to the PSMA coated chip.

LSPR, briefly:

Wrinkled gold surface polystyrene chips, with conjugated pCB, were coated in PSMA protein (via EDC/NHS chemistry) and washed with TRIS and PBS buffers. Next a non-targeting (NT) MuTE was incubated with the chip and absorbance and peak shift were measured for association and dissociation (NT-MuTE removed). The surface was rinsed thoroughly with PBS and the targeting MuTE was applied and absorbance and peak shift were measured for association and dissociation.

OKT3-(EO)$_{12}$-GUL (22/Ab)
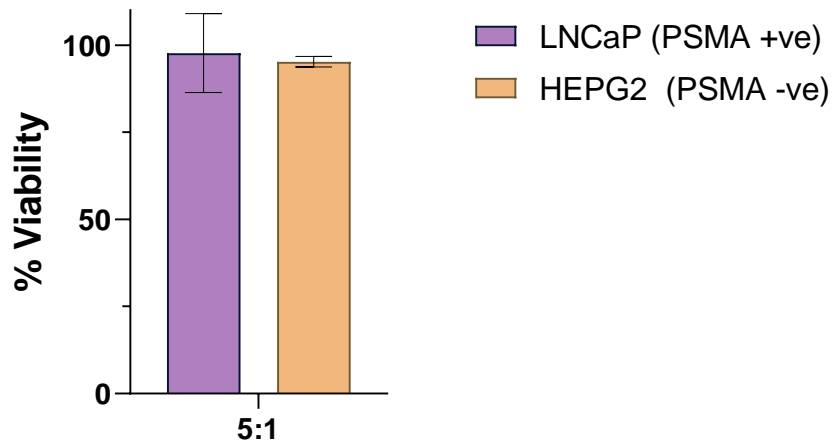
0.3 Figure S3. Highly grafted MuTEs.

EO$_{12}$ GUL MuTEs with a large amount (22) of EO-GUL units perform poorly. Comparison of PSMA Positive LNCaPs and PSMA Negative HEPG2, 5:1 E:T Ratio at 1 nM, n=3 mean ± SD
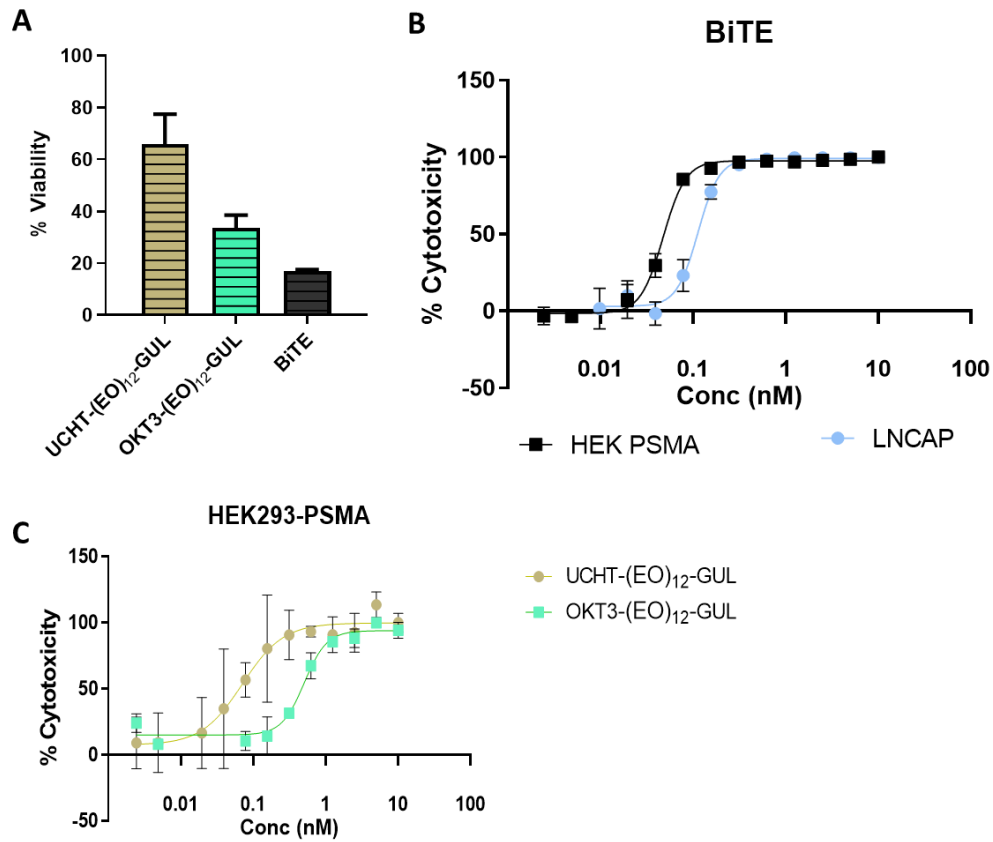
0.4 Figure S4. HEK-PSMA responds to PSMA targeting T cell Engagers.

A) 1 nM comparison of PSMA MuTEs and PSMA BiTE in HEK-PSMA cells. 5:1 E:T Ratio, n=3 mean ± SD. Dose response curves for B) HEK-PSMA and LNCaP against PSMA BiTE and C) HEK-PSMA against two PSMA MuTE structures. 5:1 E:T Ratio, n=3 mean ± SEM.
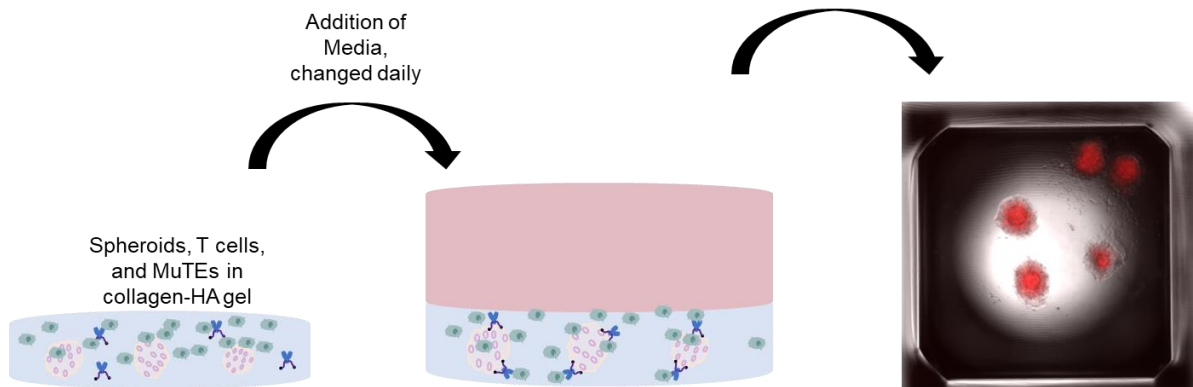
0.5 Figure S5 Schematic or 3D spheroid assay set up.

Magnification of 1.25x in brightfield and Cy5 overlayed for representative image of whole well in 384 well plate.